UNITED STATES DEPARTMENT OF THE INTERIOR
GEOLOGICAL SURVEY

HYDROCARBON RESOURCE REPORT FOR PROPOSED OCS SALE NO. 83 NAVARIN BASIN, ALASKA

by

M. S. Marlow, P. Carlson, A. K. Cooper, H. Karl,
H. McLean, R. McMullin, and M. B. Lynch

Open-File Report 81-252

1981

ILLUSTRATIONS

TABLES

TABLE OF CONTENTS

SUMMARY

Recent seismic-reflection surveys reveal a frontier province of exceptional size--the Navarin basin province--beneath the northwestern Bering Sea shelf. Structure contours drawn on acoustic basement define three basins within the province; the basins contain strata 10 to 15 km thick and underlie more than 45,000 km^2 (11 million acres) of the Bering Sea shelf.

Tertiary mudstone dredged from the continental slope averages more than 0.33 percent (range of .33 to .88) organic carbon, and Cretaceous mudstone along the continental slope in Pribilof Canyon contains as much as 1 percent organic carbon. However, these mudstones may not be correlative with the lower sequences in the Navarin basin because the stratigraphically lower beds wedge out against the flanks of the basin.

Eocene to Pliocene diatomaceous mudstones exposed on the continental slope have porosities ranging from 14 to 68 percent (average, 48 percent). Neogene reservoir beds may be present in the adjacent Navarin province because sedimentation has matched subsidence, which averaged 100 to 200 $m/10^6$ yr during Cenozoic time. Also, during Neogene time the Navarin basins were fed by major Alaskan and Siberian rivers, e.g., the Yukon, Kuskokwim, and Anadyr rivers.

Large anticlinal structures in the northern half of the province that may have diapiric cores, structures associated with growth faults along the flanks of the basins' strata draped over basement blocks, and stratigraphic pinch outs and discordances in

exploration, including the drilling of stratigraphic test wells is needed to define this frontier province.

Geologic processes in the Navarin basin province include several which are potentially hazardous to commercial development. Although the Navarin basin province presently appears to be aseismic and no faults mapped to date rupture the sea-floor, several faults indicate movement in the last 12,000 years and, thus, are potentially active. Submarine landslides evince unstable sediment masses in the heads of Zhemchug, Pervenets, and Navarinsky submarine canyons and on the continental slope. Large sediment waves in the heads of these canyons could be hazardous if active. Intense storms produce exceptionally large waves which are not only capable of eroding bottom sediments, but also are dangerous to surface structures and vessels. Gas-charged sediment, present throughout a large part of the basin, has reduced strength and bearing capacity as compared to strength of gas-free sediment. Volcanic activity is a hazard of low probability. Migratory pack ice is a yearly occurrence and could pose a significant problem during years of heavy concentrations.

INTRODUCTION

Location of Proposed Lease Area

This report is a summary of data concerning the Navarin basin province and the surrounding portion of the northern Bering Sea shelf. The proposed lease area is bounded on the north by 63°N latitude, on the northwest by the U.S.-Russia Convention Line of 1867, on the east by the 174°W meridian, on the south by 58°N latitude, and on the southwest by the 2400-meter bathymetric contour defining the base of the slope of the Bering Sea (Beringian) continental margin (Fig. 1).

The authors thank John Barron, Robert Arnal, and Paula Quinterno of the U.S. Geological Survey and Hugh Wingate of Cities Service Co. for identifying fossils from dredge samples. Jeffrey Fischer, Kenneth Johnson, David M. Jones, Margaret Kingston and Beth Lamb, prepared the illustrations and assisted with the text. Dorothy Sicard and La Vernne Hutchison processed the manuscript.

Publicly Available Data

Recent interest in the resource potential, including the hydrocarbon prospects of the Bering Sea, has stimulated marine geophysical and geologic mapping of the area. Since 1970 the U.S. Geological Survey has conducted numerous expeditions to the Bering Sea, and three of these cruises resulted in the collection of more than 970 km of 24-channel seismic-reflection data over the northwestern Bering Sea shelf in the vicinity of the Navarin basin province (Fig. 2). Data presented in this report were

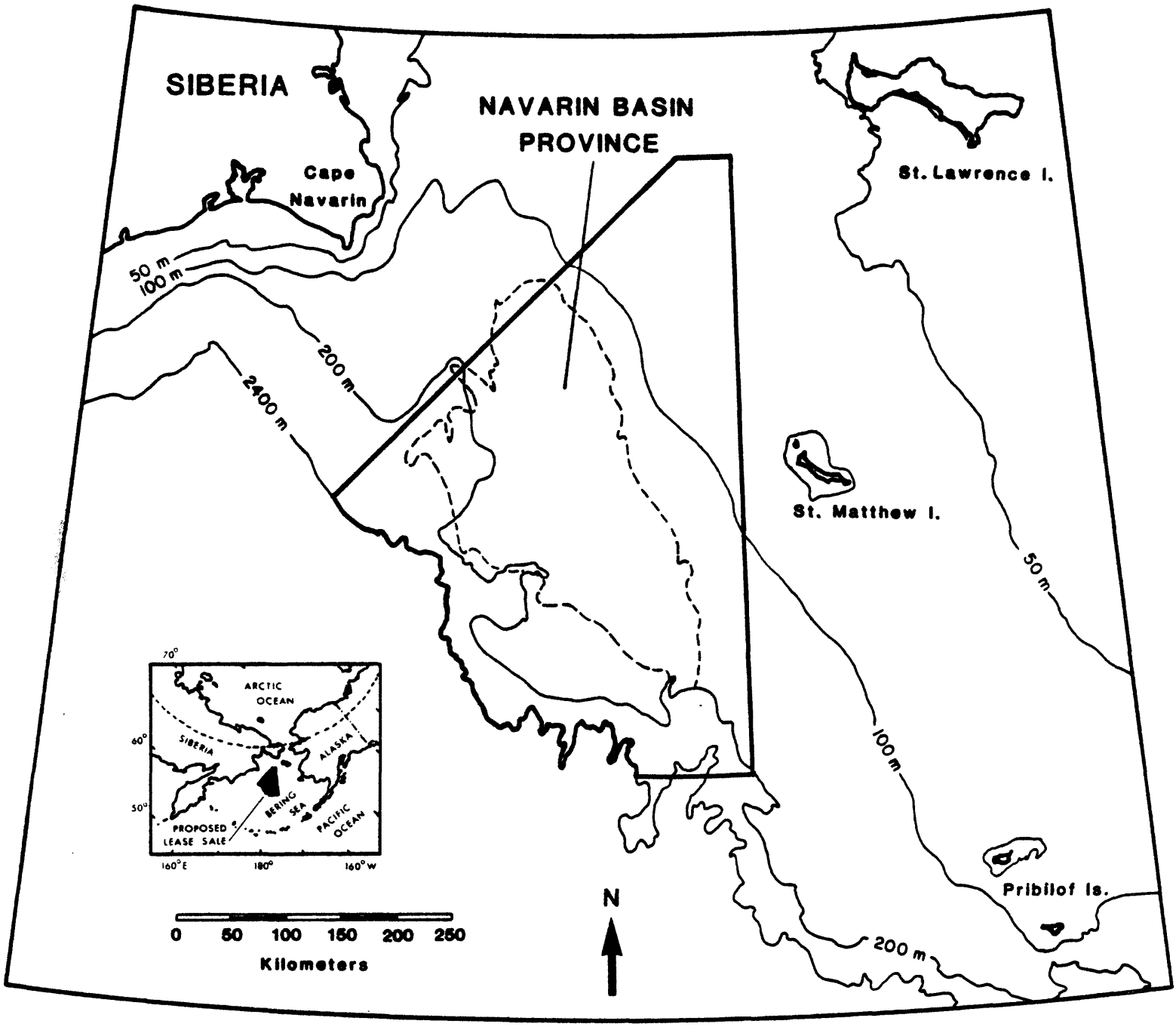

Figure 1. Location of proposed OCS Lease Sale #83 in the northern Bering Sea. Albers equal area projection.

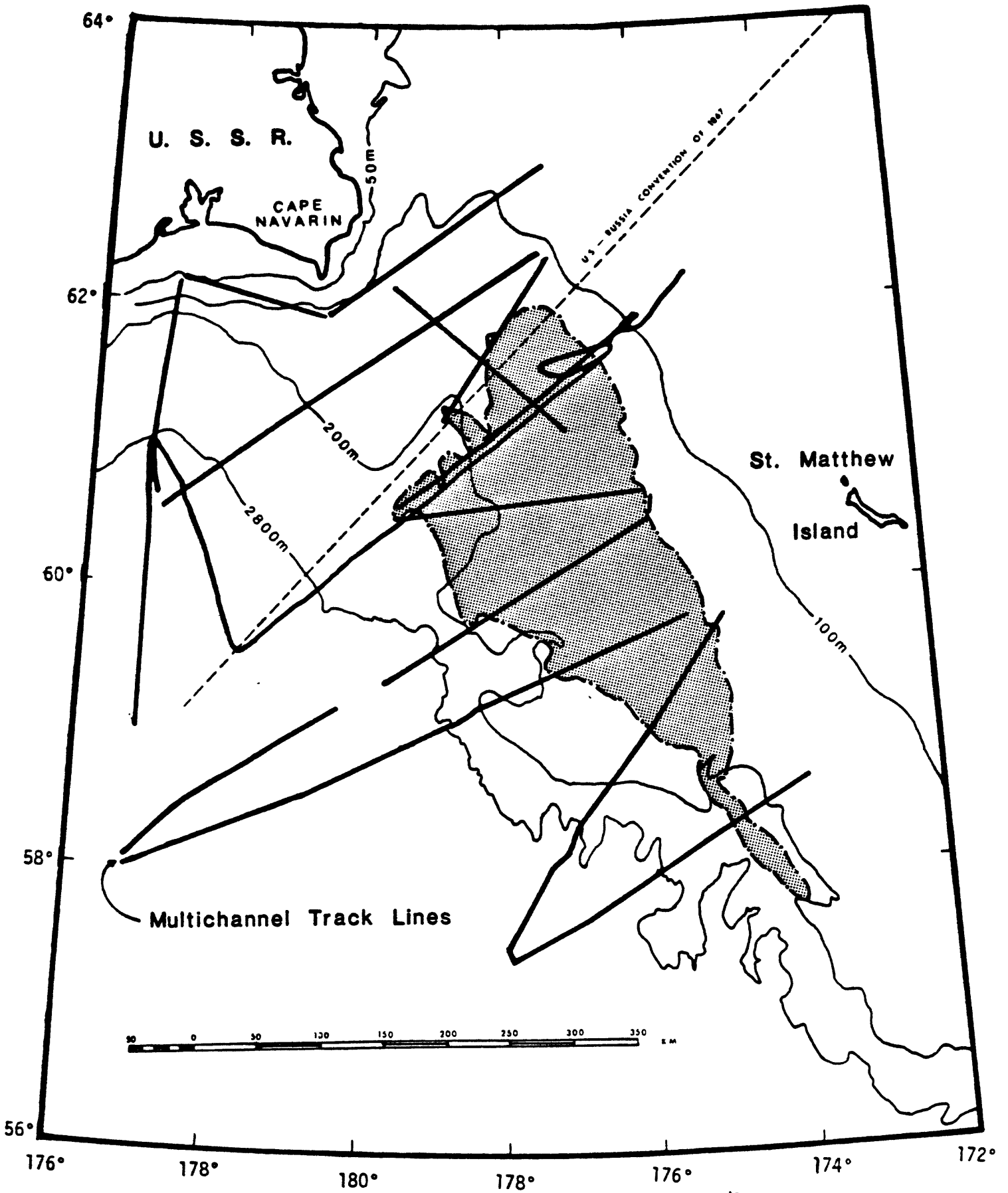

Figure 2. Trackline chart of 24-channel seismic reflection profiles across the Navarin basin province. High resolution seismic reflection, refraction, bathymetry, gravity, and limited magnetic data were also collected along the tracklines. Navarin basin province shown by stipple pattern. Albers equal area projection.

derived in part from 24-channel seismic-reflection profiles that were collected using an array of five airguns (1,326 cu. in.; 21,723 cc) as a sound source. A detailed bathymetric chart of the shelf area by R. Pratt and F. Walton (Bathymetric Map of the Bering Shelf, 1974) is available from the Geological Society of America, Inc., 3300 Penrose Place, Boulder, Colorado 80301. Additional offshore geophysical data may be obtained from the National Oceanic and Atmospheric Administration, Environmental Data and Information Service D6, National Geophysical and Solar-Terrestrial Data Center, Boulder, Colorado 80303, and the Lamont-Doherty Geological Observatory, Columbia University, Palisades, New York.

The following sections include discussions of regional geology, petroleum geology, environmental hazards as background to discussion of the hydrocarbon potential, and resource appraisal of the offshore area. A section on the technology and manpower needed and available for development of offshore resources is also included. Much of this report was derived from previously published reports by Marlow and others (1976, 1979a, b), McLean (1979a), Marlow (1979), and Marlow and Cooper (1980).

FRAMEWORK GEOLOGY

Regional Geologic Setting of the Northwestern Bering Sea Shelf

A generalized geologic map of the onshore eastern Bering Sea region is shown in Figure 3. Detailed discussions of the geology of the Alaska Peninsula can be found in Burk (1965), Brockway and others (1975), Lyle and others (1979), and McLean (1979b), of

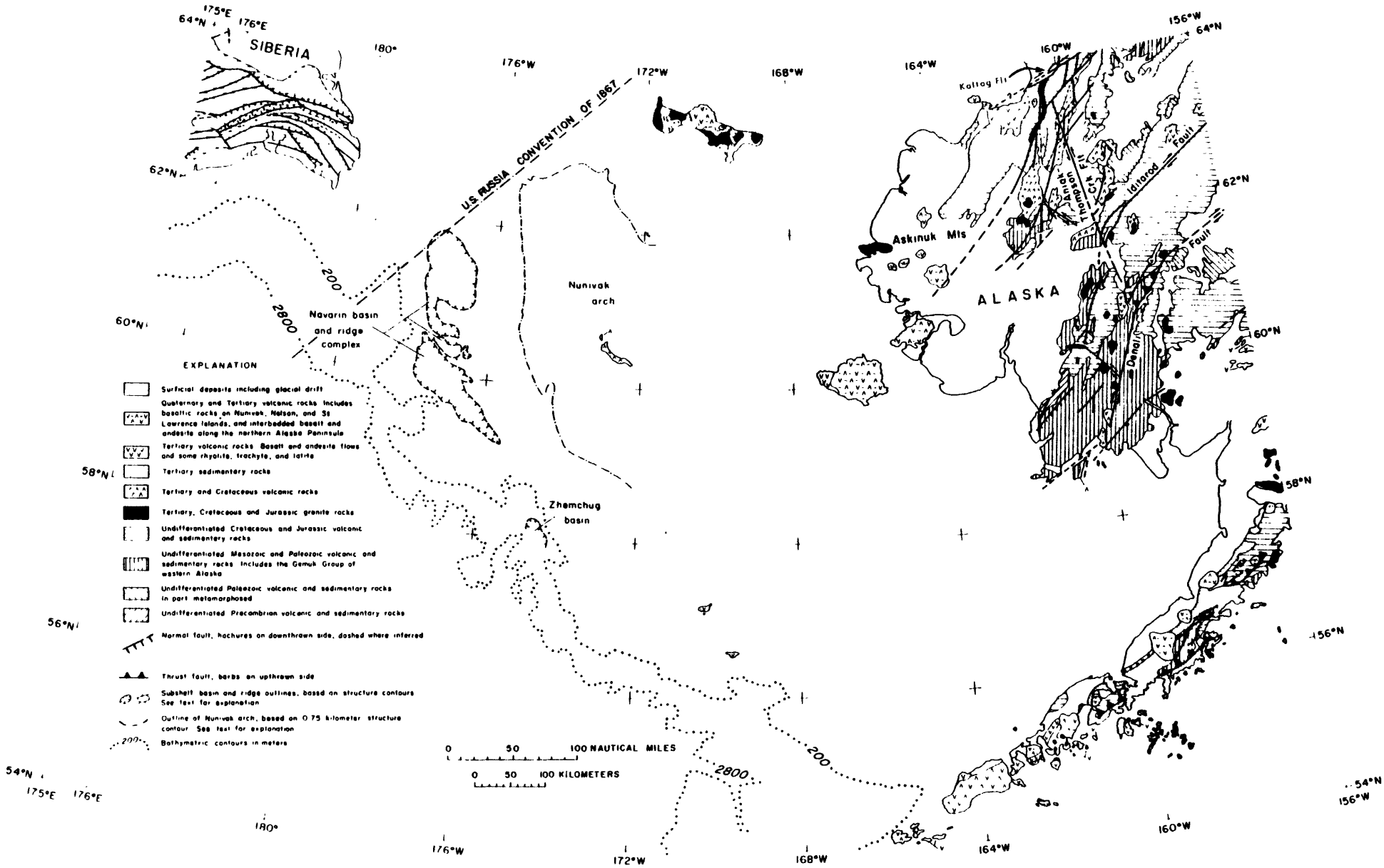

Figure 3. Generalized geologic map of the western Alaska, the Alaska Peninsula, and eastern Siberia. Onshore geology is modified from Burk (1965), Beikman (1974), and Yanshin (1966).

western Alaska in Hoare (1961) and Patton (1973), of St. Lawrence and St. Matthew Islands in Patton and Csejtey, (1971), and Patton and others, (1976), and of eastern Siberia in Churkin (1970), Scholl and others (1975), Aleksandrov (1973), Aleksandrov and others (1976), and McLean (1979a). For this report we will restrict our regional geologic discussion to western Alaska, St. Lawrence and St. Matthew Islands, eastern Siberia, and the offshore area of the Navarin basin province.

Geology of Western Alaska

Cretaceous and older Mesozoic eugeosynclinal rocks exposed in southwest Alaska north of Bristol Bay form distinct geologic terranes which trend southwestward toward the Bering Sea shelf (Fig. 3; Payne, 1955; Hoare, 1961; Gates and Gryc, 1963; Patton, 1973). These terranes are thought to be allochthonous tectonic fragments that were rafted into and juxtaposed against nuclear Alaska in Mesozoic and earliest Tertiary times (Jones and others, 1978). The important structural features that mark terrane boundaries either disappear to the southwest beneath the Bering shelf or they curve to the northwest and merge with the belt of shallow-water, indurated Mesozoic rocks that underlie the outer part of the Bering shelf and its margin (Scholl and others, 1975; Marlow and Cooper, 1980). We also suspect that the two major strike-slip faults of western Alaska, the Denali and Kaltag faults, either vanish to the southwest or turn to the northwest parallel to the Bering Sea margin.

Geology of St. Lawrence and St. Matthew Islands

The Navarin basin province is flanked to the east by a broad basement high, Nunivak arch, that is exposed only on St. Matthew and St. Lawrence Islands (Fig. 3; Marlow and others, 1976).

St. Matthew Island and the western part of St. Lawrence Island are underlain by a belt of upper Mesozoic to lowest Tertiary volcanic and plutonic rocks (Patton and Csejtey, 1971; Patton and others, 1976). The belt of igneous rocks extends to the northwest and underlies the southern Chukotsk and Anadyr River region in northeastern Siberia.

St. Lawrence Island is also underlain by older, unmetamorphosed Paleozoic and lower Mesozoic carbonate and nonvolcanic rocks, which are nearly identical in age and lithology to the sections exposed in the northern Brooks Range (Patton and Csejtey, 1971). Two different lower Tertiary deposits, one Paleocene and the other early Oligocene in age, crop out on St. Lawrence Island. The older sequence includes mafic, intermediate, and felsic volcanic flows and tuffs intercalated with lignitic coal beds and tuffaceous sedimentary rocks. The younger sequence contains poorly consolidated calcareous sandstone and conglomerate, carbonaceous mudstone, ash tuff, and volcanic breccias (Patton and Csejtey, 1971). Exposures of lower Tertiary rocks on St. Lawrence Island are poor and their offshore extent is unknown.

Geology of Eastern Siberia

A generalized cross section that traverses the northeastern

Koryak Mountains (Figs. 4, 5) is adapted from McLean (1979a), who in turn abstracted the section from the original work of Aleksandrov and others (1976). The eastern Koryak Range is underlain by structurally juxtaposed blocks of different age and lithology. McLean (1979a) compared the complex rock fabric of the Koryak Range to the Franciscan assemblage in California as described by various workers (e.g., Bailey and others, 1964; Hamilton, 1969; Bailey and Blake, 1969; Ernst, 1970; Page, 1970, 1978) and to the McHugh and Uyak Complexes of southwestern Alaska (Clark, 1973; Connelly, 1978; Tysdal and Case, 1976; Tysdal and others, 1977). Rock types common to all three areas include chert (red, gray, and green), siliceous shale, siltstone, fine-grained graywacke, tuff, spilite, pillow basalt, blueschist, and ultramafic rocks. The age of the graywacke in the Koryak Range is estimated as either Triassic to Early Cretaceous (Valanginian) or Late Jurassic (Tithonian) to Early Cretaceous (Hauterivian) (McLean, 1979a).

Large slablike rock bodies occur within the Koryak Mountains. These slabs are separated by northward-dipping thrust faults and include olistostrome and melange sequences (Figs. 4 and 5). At the base of many of the tectonic slabs and sheets are ultramafic masses consisting of pyroxenite, peridotite, and serpentinite associated with gabbro and diorite. These mafic and ultramafic assemblages may be part of an ophiolite suite (Aleksandrov and others, 1976). The assemblages are unconformably overlain by either siliceous sedimentary rocks of

Paleozoic age or volcanic and terrigenous deposits of Mesozoic age. Exotic blocks of serpentinite melanges and olistostromes (sensu Silver and Beutner, 1980) include shallow-water Devonian, Carboniferous, and Lower and Upper Permian limestones. Aleksandrov and others (1976) suggested that all Paleozoic deposits in the Koryak Mountains are allochthonous units that by the end of the Mesozoic were tectonically derived from the south, in the vicinity of the present-day Bering Sea. Thrusting of the allochthonous units apparently continued into early Paleogene time (Aleksandrov and others, 1976; McLean, 1979a).

Early Cretaceous magmatism in the Koryak Mountains coincided with the accumulation of olistostromes to the south toward the Bering Sea, in front of rising tectonic slabs (Aleksandrov and others, 1976). Compression and foreshortening of the Koryak Range apparently continued into Paleocene time as evidenced by isoclinally folded rocks of Paleocene age exposed on the southeast side of the range (Aleksandrov and others, 1976; McLean, 1979a). These younger deformed rocks are composed of reworked debris from older, previously deformed units of the subduction complex present in the Koryak Mountains.

STRUCTURAL FRAMEWORK AND EVOLUTION OF NAVARIN BASIN

Seismic-Reflection Data

Profile A-B

A 1,620-km-long seismic-reflection profile, A-A' (Fig. 4), transects the northwestern Beringian margin west of St. Matthew Island. An interpretive drawing of profile A-B (Fig. 6) shows

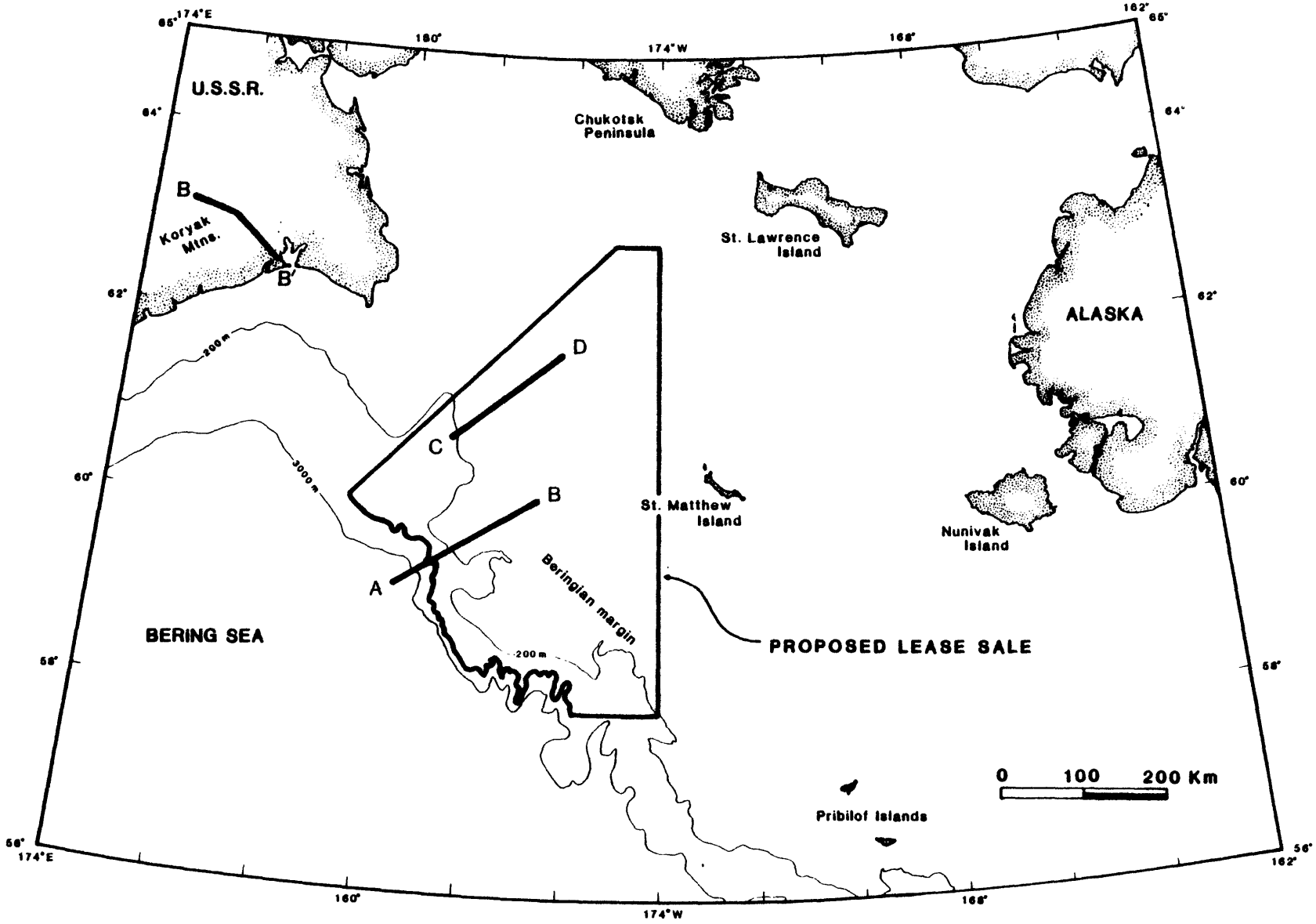

Figure 4. Location map of selected cross sections across the Navarin province and eastern Siberia shown in Figures 5, 6, and 7. Note also outline of proposed lease area. Albers equal area projection.

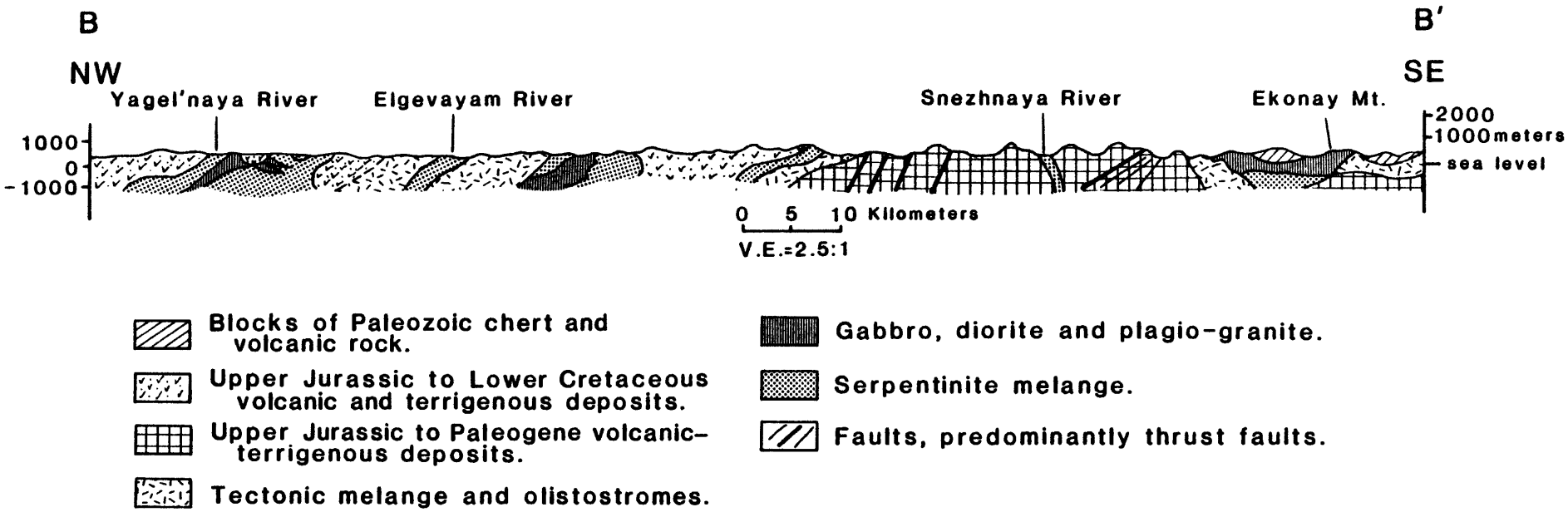

Figure 5. Generalized cross section across the Koryak Range in eastern Siberia. Adapted from Aleksandrov and others (1976) and McLean (1979a).

that the southwestern end of the profile crosses the eastern edge of the Aleutian Basin (SW end of profile) in water more than 3,000 m (4.0 sec) deep. Underlying the seafloor are 4 to 5 km of undeformed strata which overlie a distinct acoustic basement. Magnetic and refraction-velocity data indicate that the basement is oceanic crust of Mesozoic age (Kula(?) plate; Cooper and others, 1976a, b).

Below the lower part of the continental slope, the rock sequence is acoustically characterized by scattered and discontinuous reflectors (Fig. 6). Oceanic basement was not resolved. In contrast, a strong basal reflector, a subshelf basement, can be traced from the northeast seaward to the middle of the continental slope where the basement crops out. Dredged rocks and the flatness of the subshelf basement indicate that beneath the slope the shelf basement is a wave-base unconformity cut across broadly folded rock sequences of Jurassic and Cretaceous age. These dredge and seismic-reflection data attest that the subshelf basement beneath the slope has subsided at least 1,500 to 1,700 m since about Paleocene or Eocene time (Marlow and Cooper, 1980).

Basement beneath the shelf can be followed to the northeast below the thick sedimentary section filling Navarin basin (Fig. 6). Near the northeastern end of the profile, strata in the basin are nearly 12 km (7 sec) thick. Reflections from the upper basin fill are strong, continuous, and flat. Apparent breaks in the continuity of these reflectors are associated with

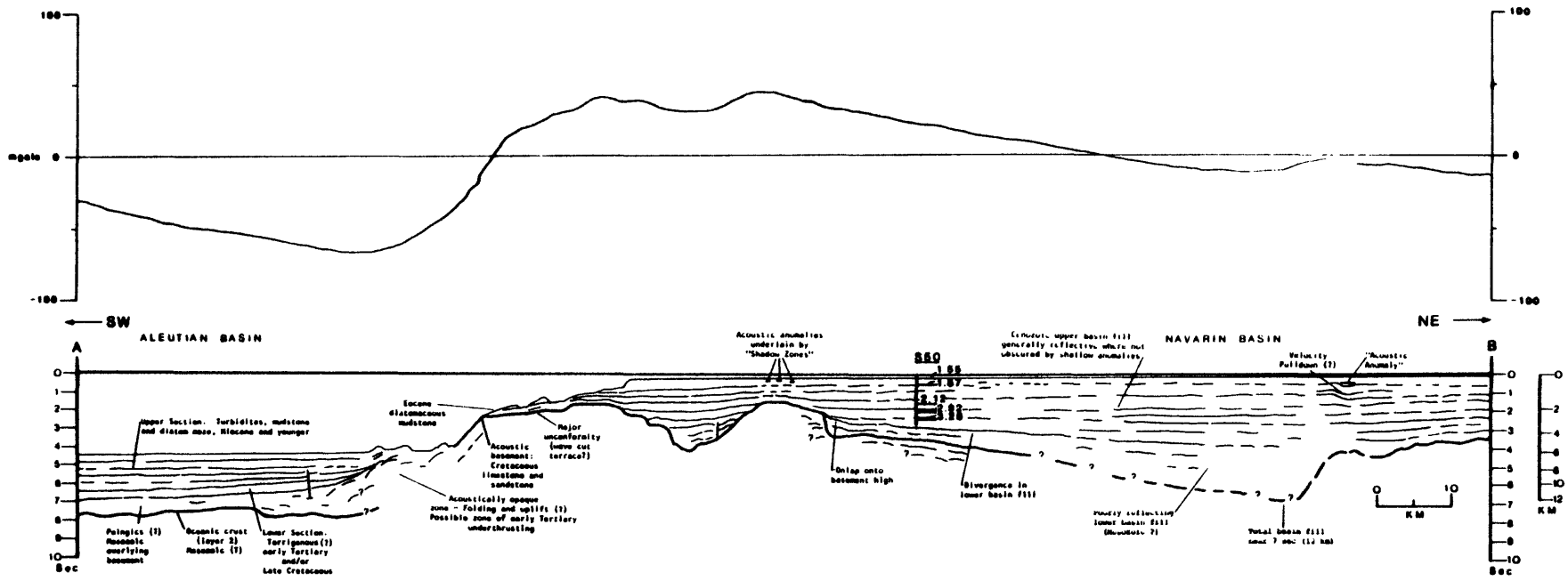

Figure 6. Interpretive drawing of seismic-reflection profile A-B across the Navarin basin province. Free-air gravity profile shown at top. Vertical kilometer scale shown at right is applicable only to the shelf portion of the profile. Vertical time scale is two-way travel time. For location of profile see Figure 4.

columnar "wipe-out" zones beneath short discontinuous reflectors in the upper few hundred meters of the section. The acoustic "wipe-out" zones are thought to be produced by shallow accumulations of gas that mask the lateral continuity of deeper reflectors (Marlow and Cooper, 1980). Dredge data indicate that the upper 3 to 4 km of the beds in the basin are younger than early Eocene. Deeper strata are poorly reflective, diverge in dip from the overlying strata, and near the base of the section may be Cretaceous or older (Marlow and others, 1976; Marlow, 1979).

Profile C-D

A second 175-km-long seismic-reflection profile, C-D (Fig. 4), crosses the northern Navarin basin province near the U.S.-Russia Convention Line of 1867. Figure 7 is an interpretive drawing of profile C-D, which shows that the northern basin in the Navarin province is 105 km wide. At the southwest end of profile C-D, acoustic "basement," or what we informally term the "bedrock" reflecting horizon, can be traced to the northeast as a prominent reflector 2-3 km deep. Near the central portion of the profile, the basement horizon plunges deeper than 7 seconds (two-way time), indicating that the basin fill is thicker than 12 km. To the northeast acoustic basement rises to within a few hundred meters subbottom. Here the bedrock reflector appears to be beveled and may be part of a wave-cut surface. The sedimentary section flanking the basement reflector is broadly folded, faulted, and cut by a major unconformity that is

contiguous with the beveled portion of the basement (Fig. 7).

The upper sequence of reflectors in Navarin basin are generally highly reflective and continuous, except where the reflection events are interrupted by columnar "wipe-out" zones thought to be associated with shallow accumulations of gas (Fig. 7; see discussion of profile A-B). In contrast, the lower section in the central portion of Navarin basin is poorly reflective and discontinuous. The lower sequence along the southwestern flank of Navarin basin diverges in dip from the overlying strata and appears to pinch out against the flank of the basin. The lower sequence in Navarin basin may be poorly reflective because the lower fill may be composed in part of coarse, locally derived clastics shed into the early depocenter of Navarin basin (Marlow and others, 1976).

The reflective upper sequence is gently folded into broad arches that may be anticlines and thus possible traps for hydrocarbons (Fig. 7). The upper few hundred meters of sediment along the entire length of profile C-D are flat lying and undeformed, and these uppermost deposits cover the major unconformity along the northeast part of profile C-D (Fig. 7). This shallow section is probably very young and may have been deposited during rising sea level.

Structure Contours

In 1970 approximately 1,000 km of single channel seismic-reflection records, using a 160-kJ sparker sound source, were collected in the Navarin province (Scholl and others, 1970). The

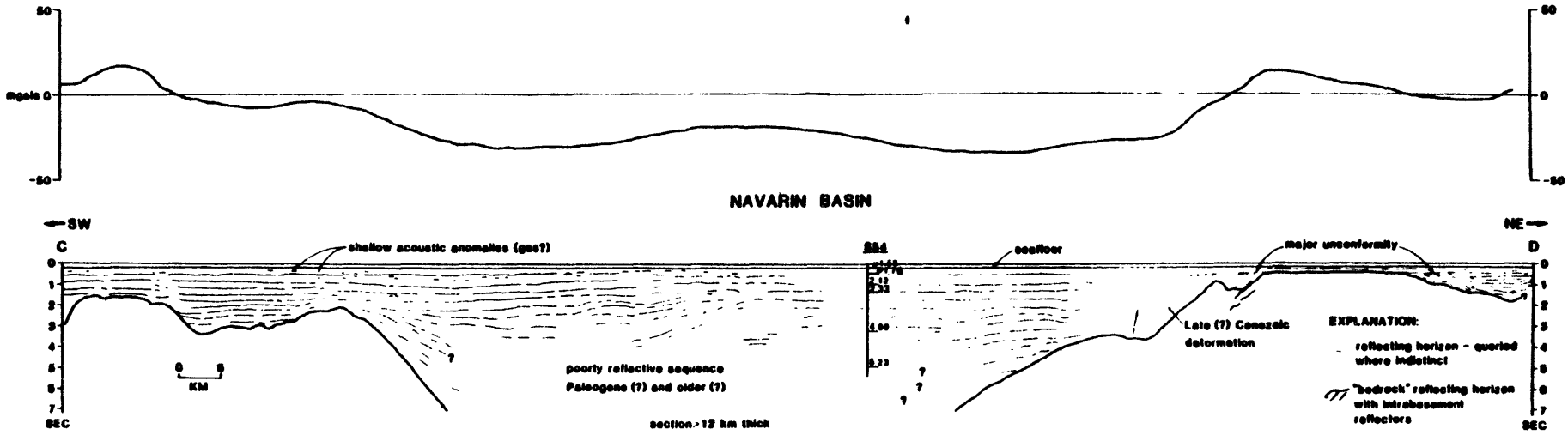

Figure 7. Interpretive drawing of seismic-reflection profile C-D across the Navarin basin province. Free-air gravity profile shown at top. Vertical time scale is two-way travel time. For location of profile see Figure 4.

reconnaissance records indicate that a thick stratified section underlies the northwestern Bering Sea shelf. Therefore, in their report based on these data, Marlow and others (1976) could give only a rough outline of the basin province. During 1976, 1977, and 1980 surveys, 970 km of 24-channel seismic-reflection data were collected over the basin province proper using a sound source of five air guns totaling 1,326 in^3 (Fig. 2). These data allowed us to construct the structural contours of "acoustic basement" shown in Fig. 8.

The multichannel data revealed that the Navarin basin province comprises a series of northwest-trending basins and ridges (Fig. 8) and that the stratified sequence in the basins is 10 to 15 km thick. To convert two-way travel time on the seismic-reflection records to depths in meters or kilometers, we used a generalized velocity function.

$$D = 1.266t + 1.033t^2 - 0.117t^3$$

where

D = Depth or thickness in km

t = One-way travel time

This function was derived by fitting a polynomial curve to velocity data from 150 sonobuoy stations in the Bering Sea. The velocity function used here supersedes the curve published by Marlow and others (1976).

The structure contours of acoustic basement indicate that the Navarin basin province actually comprises three filled basins each separated by basement ridges that trend to the northwest

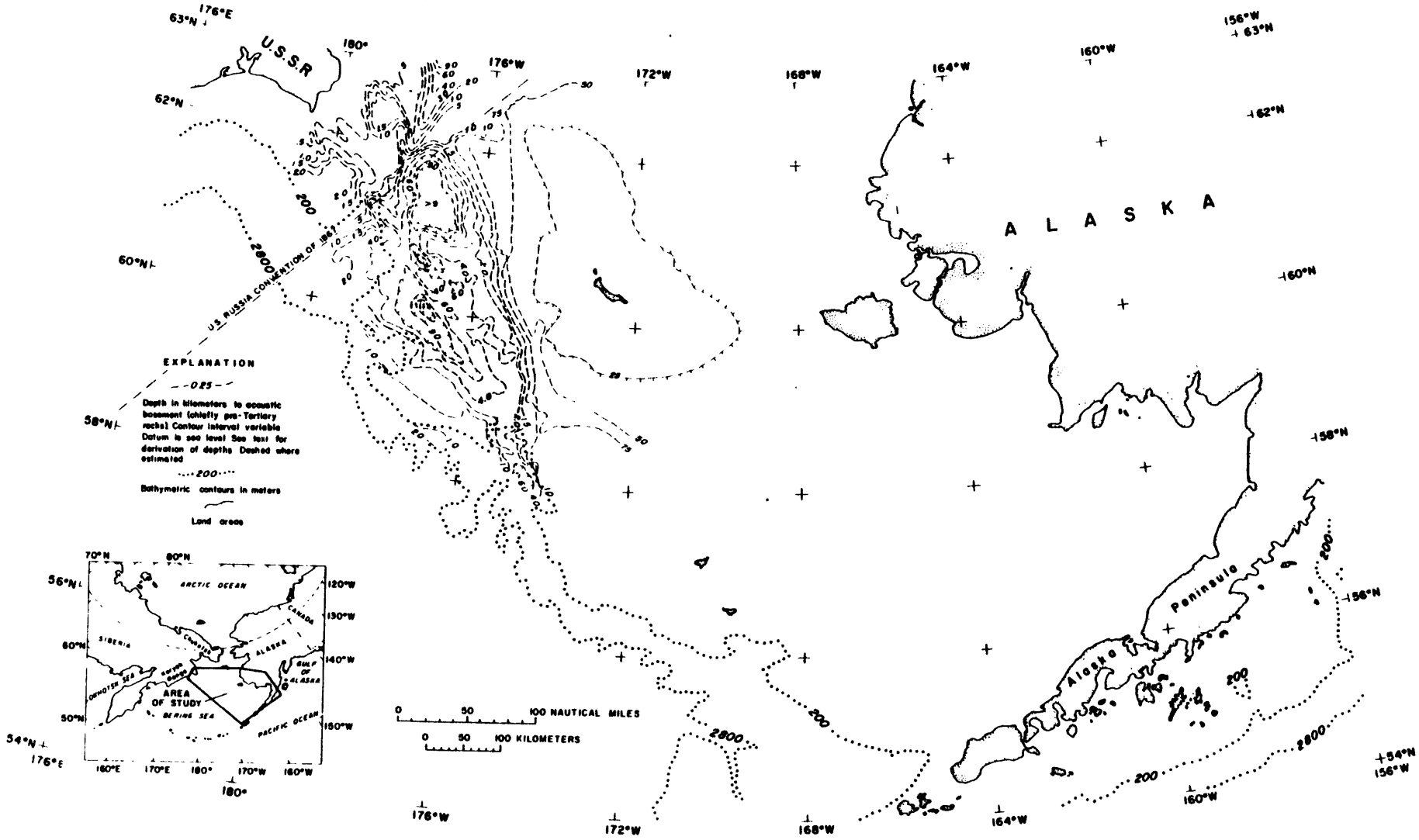

Figure 8. Structure contour map of acoustic basement in the Navarin basin province. See text for details of derivation. Albers equal area projection.

parallel to the adjacent Beringian margin (Fig. 8). The southern basin is a filled elongate trough some 200 km long (7,700 km^2; 1,902,500 acres in area) that is on strike with Zhemchug Canyon and Zhemchug basin (Fig. 3), a partially filled basin just south of the Navarin basin province (Marlow and others, 1976). The southern basin is filled with more than 11 km of strata that are broken by normal faults along the basin flank that exhibit growth structures (Marlow and Cooper, unpublished data).

The central basin in the Navarin province, like the southern basin, is also an elongate and filled depression that trends to the northwest (Fig. 8). The central basin is smallest of the three basins and encompasses an area of 1,500 km^2 (370,500 acres).

A large circular basin underlies the northern Navarin basin province adjacent to the U.S.-Russia Convention Line of 1867 (Fig. 8). The northern basin is the largest feature in the province, covering an area of 10,350 km^2 (2,557,450 acres) and containing 12-15 km of sedimentary section. Near the 1867 Convention Line, strata in the basin are folded into large anticlines 10-15 km across that may have diapiric cores (Marlow, 1979). These fold structures may be prospective traps for hydrocarbons.

Geologic History

The geologic history of the Navarin basin province is poorly known owing to the lack of subsurface samples from the basins. The province has been covered fairly extensively by geophysical

surveys, allowing the delineation of major basins in the area as well as major structures capable of trapping hydrocarbons. One or two COST (Continental Offshore Stratigraphic Test) wells are to be drilled in the province in 1981 and 1982.

Mesozoic Structural Trends

Regional geophysical surveys of the entire Bering Sea shelf coupled with dredging of the adjacent continental margin have allowed the delineation of major Mesozoic structural trends beneath the outer Bering Sea shelf (Marlow and Cooper, 1980). Upper Jurassic sandstone units of the Naknek formation are exposed near the western tip of the Alaska Peninsula where they crop out in the Black Hills (Burk, 1965). These Jurassic rocks can be traced offshore as bedrock ridges along the entire Bering Sea margin. Seaward of Navarin basin exposures of these structural highs have yielded dredge samples of Late Jurassic or Early Cretaceous, and Late Cretaceous age. Many of the structural highs appear on seismic-reflection records as beveled terraces that have subsided several kilometers. The very thick sedimentary section filling the adjacent basins in the Navarin basin province suggests that the early depocenters of the province may contain late Mesozoic strata. These strata may have been shed by the nearby structural highs, which would have been exposed as flanking islands, mountains, and peninsulas during the initial subsidence of the Navarin basin province.

Cenozoic Subsidence

Dredge samples from near the base of the section overlying

the structural highs which flank the Navarin basin province are early Tertiary (Paleocene to Oligocene) in age (Marlow and Cooper, 1980). While it is difficult to trace the early Tertiary section into the basins in the Navarin province, we suspect that a fairly thick lower Tertiary section fills the basins. The dipping strata observed in the basins' lower fill are probably in large part early Tertiary in age. The relatively flat-lying overlying section is probably Miocene and younger. In places, the upper section is broadly folded and truncated, especially in the northern end of the province. This period of deformation may be related to late Miocene and Pliocene uplift and folding in the nearby Koryak Mountains of eastern Siberia.

In summary, basins in the Navarin province probably contain a fairly complete Cenozoic section and may contain lower units as old as late Mesozoic in age. Subsidence has apparently continued throughout the Cenozoic and may still be active.

PETROLEUM GEOLOGY

The following section on petroleum geology is divided into two parts: the first part describes the petroleum potential and Soviet exploration of two large sedimentary basins in eastern Siberia, Anadyr and Khatyrka basins, and is abstracted from McLean (1979a); the second part discusses petroleum potential of samples dredged from the continental margin adjacent to Navarin basin, and is abstracted from Marlow (1979) and Marlow and others (1979c).

Anadyr Basin

Anadyr basin is a large (approximately 100,000 km^2) structural depression filled with Upper Cretaceous and Tertiary sedimentary rocks. The onshore part of the basin underlies the Anadyr Lowlands and is flanked on the north, west, and south by folded Mesozoic rocks of the Koryak foldbelt (Fig. 9). To the east and southeast, the basin extends offshore as far as 200 km (Fig. 9). The basin covers approximately 35,000 km^2 onshore and nearly 60,000 km^2 offshore. The deepest parts of the basin contain at least 6 km of mildly deformed terrigenous sedimentary fill (Verba and others, 1971).

Seismic-reflection and gravity data show approximately 50 northeast-trending anticlinal structures onshore that range in size from 5 to 7 km wide and 7 to 10 km long. Dips are generally low (2° to 3°) in the upper beds of these structures but increase to 40° or more at depth, indicating syndepositional uplift and the development of growth faults. The basin also contains deep grabens, the upthrown sides of which are half-anticlines with gentle flanks dipping into the faults; there are also unfaulted uplifts that have gentle flanks on one side and steep flanks on the other (McLean, 1979a). Offshore reconnaissance geophysical work by the Soviets has defined a large southeast-trending structure known as the East Anadyr trough, a sediment-filled depression at least 90 km long (Fig. 9). The East Anadyr trough flanked on the northeast by the Okhotsk-Chukotsk belt of volcanic

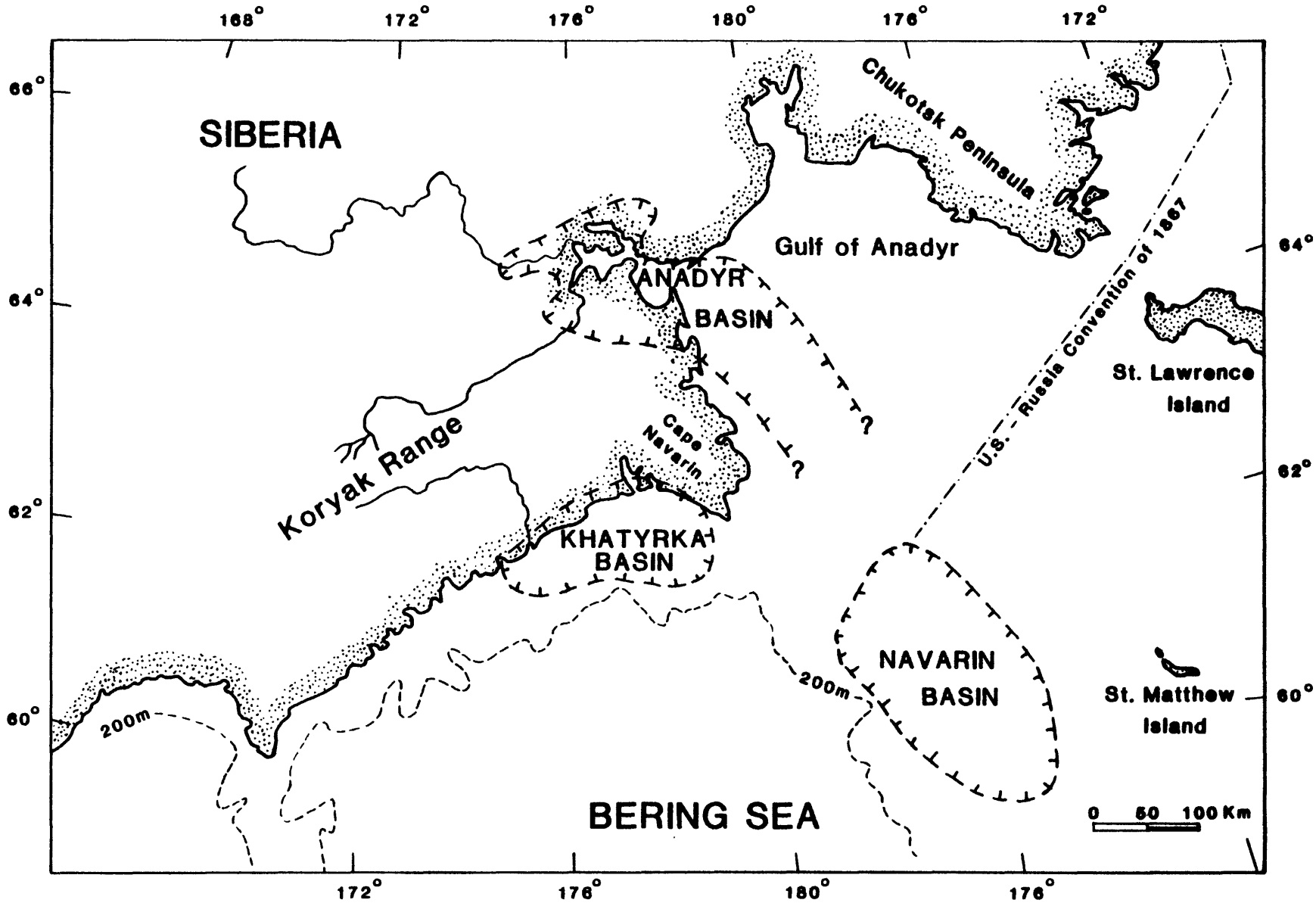

Figure 9. Location map of Anadyr and Khatyrka basins in eastern Siberia in relation to the Navarin basin province. Albers equal area projection.

and plutonic rocks (Verba and others, 1971).

Recent seismic-reflection surveys of Anadyr and Navarin basins indicate that the two basins are not connected, but are separated by a basement high that trends northwest-southeast (Marlow and Cooper, 1980, unpublished data).

Geologic and geophysical investigations of the Anadyr basin as related to petroleum potential were begun in 1959. By 1973, 20 wells had been drilled into the onshore part of the basin (locations of all but two wells are given in Soviet literature); 11 were so-called stratigraphic tests, 9 were exploratory attempts. The first exploratory well was drilled in 1969. Two later wells were drilled in 1969-70 within 13 km of the first well in the central part of the basin. A Neogene section 1,537 m thick produced excellent initial shows of gas (95 percent methane). Ten sandstone beds with 80-m aggregate thickness drilled in the middle to upper Miocene section between 867 and 1,467 m had dry porosities of 20 to 26 percent and permeabilities of 92 to 560 md (Agapitov and others; 1970; Burlin and others, 1975). Initial testing of the Vostochno-zero gas zones produced 7,000 to 10,000 Mcf/day; continued testing, however, led to sharp drops in pressure and volume (Meyerhoff, 1972).

Tests on the Zapadno-Ozero structure 13 km west were less productive (Agapitov and others, 1971). In late 1975, a well drilled in the Anadyr basin produced 100,000 cu m/day (3.5 MMcf/day) of gas from Neogene sandstone (Rovnin and others, 1976).

Further exploratory drilling in the Paleogene section has produced oil and gas shows in Eocene and Oligocene strata (Ya. N. Grigorenko, K. K. Makarov, I. S., written communication, 1974), and one well produced 0.3 ton of oil/day (approx. 2 bbl/day) from fractured strata (fracture porosity). One well, located on a structural uplift in the center of the basin, penetrated 1,020 m of Upper Cretaceous clastic rock; oil shows in the well were also noted in upper Eocene and Oligocene strata between 1,400 and 2,132 m (McLean, 1979a).

Structural traps in the Anadyr basin are predominantly anticlinal folds that exhibit low-amplitude closure over large areas. Structures in the central part of the basin are associated with uplifted blocks of basement rock. As a result, the degree of folding formed by draping of the Upper Cretaceous to Neogene section diminishes upward so that Pliocene deposits are almost undeformed. Along the southern edge of the basin, linear anticlinal structures were apparently formed by compressional folding.

Values as high as 26 percent effective porosity and 560 md permeability have been reported for some Miocene sandstone beds. The net thickness of porous sandstone reported is as much as 80 m. Rapid decrease in gas pressure during open-hole tests suggests that many sandstone beds are lenticular and that each zone contains a relatively small volume of highly pressurized gas and/or gas condensate.

Results of exploratory drilling in Anadyr basin are somewhat

similar to results in Bristol Bay basin along the northern shore of the Alaska Peninsula. In both areas, at least 10 exploratory wells have been drilled into Neogene rocks with disappointing results. However, there is speculation that hydrocarbon potential may be greater offshore, primarily because thicker sections are more deeply buried, thereby enhancing the probability of hydrocarbon maturation.

Khatyrka Basin

Khatyrka basin is south of the Koryak Range between Cape Navarin and Cape Rubicon (Fig. 9). Reconnaissance seismic-reflection data indicate that this basin encompasses an area of approximately 40,000 km^2, most of which is offshore along a narrow part of the Bering Sea shelf. The basin axis trends from east to west and contains more than 30 small anticlinal structures that trend in a northeasterly direction (Review of Sino-Soviet Oil, 1974). A northward trending basement high divides the basin into two subbasins, each containing at least 4 km of sedimentary fill and possibly as much as 7 to 8 km. Only the northern edge of the basin (about 4,000 km^2) is exposed onshore.

Anticlinal structures within the Cenozoic fill of Khatyrka basin are generally oval (3 to 4 km by 5 to 6 km). Locally, the fold axes strike northwestward, and some of the structures have diapiric upwellings of Paleogene clay (Review of Sino-Soviet Oil, 1974).

Exploration in Khatyrka basin was stimulated by the

discovery of onshore oil seeps and more than 200 hydrogen sulfide springs emanating from Miocene rocks (Trofimuk, 1971). Upper Cretaceous and Paleogene rocks reportedly contain solid hydrocarbon inclusions (ceresins and asphaltites) and Oligocene claystone beds contain gypsum and carbonate concretions with veins colored by bitumen.

Geochemical data from Khatyrka basin suggest greater hydrocarbon potential than in Anadyr basin (Burlin and others, 1975). Analyses of upper Senonian marine shale from the basin indicate that the total organic carbon (TOC) content ranges up to 0.81 wt. percent (0.04 percent extractable bitumen). Insoluble kerogen in these strata is predominantly humic.

The Eocene and Oligocene sequence contains argillite that has an average TOC content of 1.05 percent and 0.06 percent extractable bitumen. Soviet geologists suggest that source rocks in this sequence are in "the main zone of oil generation" (Review of Sino-Soviet Oil, 1974). Shale beds overlying the lower Miocene section contain sapropelic kerogen and a minor proportion of humic material. The TOC content ranges from 0.38 to 1.79 wt. percent and averages about 0.80 wt. percent. Vitrinite reflectance data from shale indicate a weak to moderate thermal history. Significant oil generation may have occurred in this sequence.

Middle and upper Miocene rocks are composed primarily of sandstone and conglomerate; shale forms thin layers. Prospective source rocks in this sequence are low in TOC, averaging about

0.02 wt. percent. Kerogen is predominantly humic, and extractable bitumen values are low, averaging about 0.02 percent. This part of the sequence is not thought to have generated significant quantities of oil (Review of Sino-Soviet Oil, 1974). Samples analyzed, however, are from outcrops or shallow core holes around the basin margin and are not representative of middle and upper Miocene strata in the more deeply buried parts of the basin. The conclusion of Burlin and others (1975) is that upper Senonian, Paleogene, and lower Miocene strata in Khatyrka basin all contain source rocks capable of oil generation interbedded with reservoir-quality sandstone. They consider these rock sequences to be highly prospective for oil and gas. A recent gas find made near Khatyrka in the Onolskaya well flowed up to 1.06 MMCf/day from three intervals in Oligocene sandstone beds (Rovnin and others, 1976). The location of the well was not reported.

Petroleum Geology of Dredge Samples Adjacent to Navarin Basin Province

Source Beds

Navarin basin province has not yet been drilled or sampled; thus, little is known about possible source beds in the province's sedimentary section. Rocks dredged from the Beringian continental slope west and southeast of the Navarin basin province include lithified volcanic sandstone of Late Jurassic age, mudstone of Late Cretaceous age, and less consolidated deposits of early Tertiary age (Fig. 10). Geochemical analyses and the physical properties of some of these rocks are listed below:

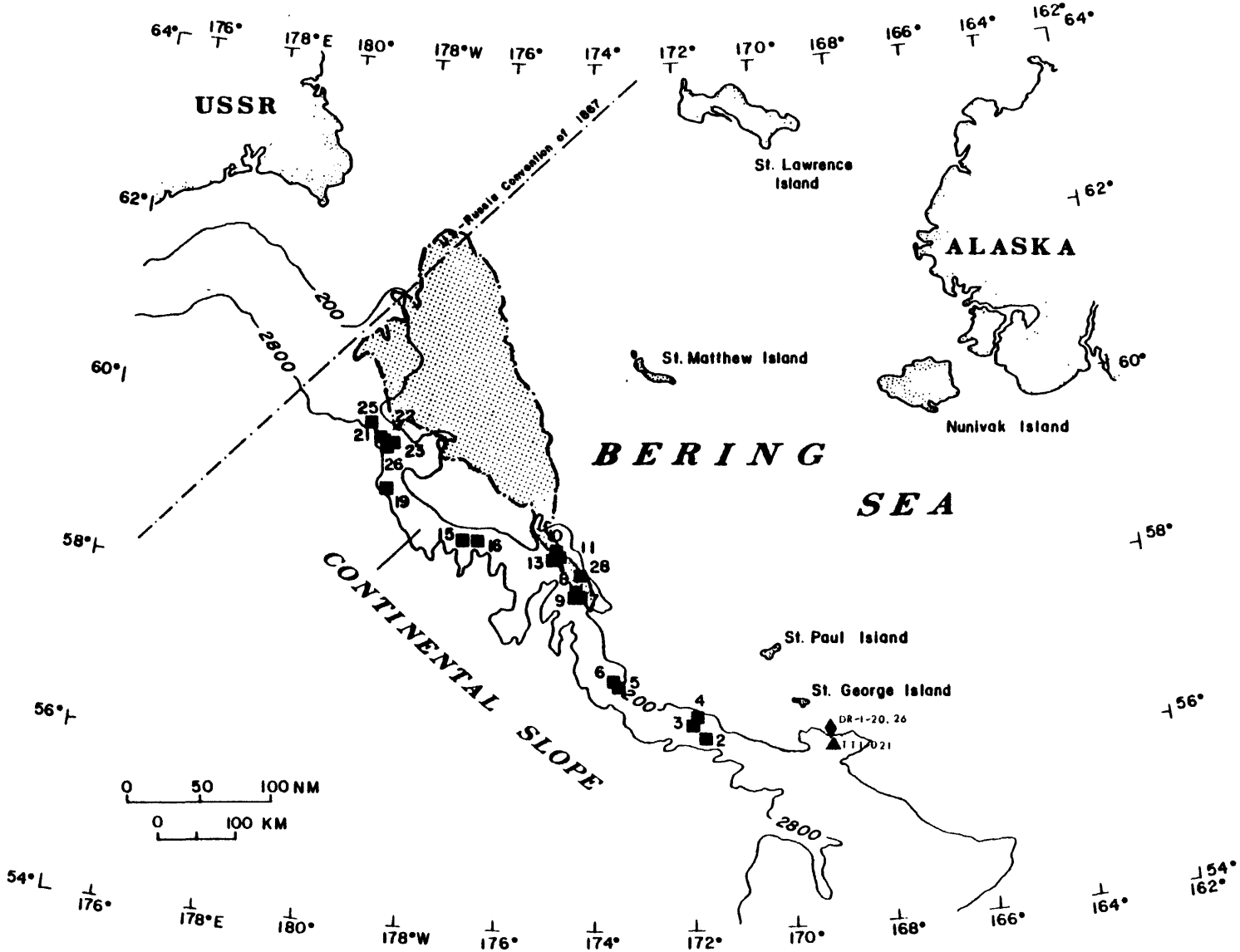

Figure 10. Location of dredge sites along the Bering Sea continental margin in relation to the Navarin basin province. Site #TT-1-021 from Hopkins and others (1969) and sites #DR-1-20, 26 are from Vallier and others (1979). Remaining sites are described in Marlow and others (1979a) and Marlow and Cooper (1980). Navarin basin province shown by stippled pattern. Albers equal area projection.

Table 1. Geochemical analyses and physical properties of rocks dredged from the Bering Sea continental margin. See Figure 10 for locations.

Sample number	Lithology	Age	Organic carbon (Wt.%)	Pyrolytic hydrocarbon (Wt%)	Vitrinite reflectance (Avg. %)	Porosity (%)/ perm.(md)
S6-77-BS						
DR1-20	Volcanic sandstone	Late Jurassic	0.79	0.24	.38	----/----
DR1-26	Volcanic sandstone	Late Jurassic	0.26	0.01	1.14	----/----
TT-1-021						
001	Mudstone	Late Cretaceous	0.62	0.22	.40	----/----
L5-78-BS						
5-5	Sandstone	L.Jurassic	.27	.02	.63	----/----
2-3	Mudstone	Paleogene	.33	.02	.41	----/----
16-9	Mudstone	M.Eocene	.83	.04	.31	----/----
2-4	Mudstone	L.Oligocene	-	-	-	68.3/5.46
2-11	Siltstone	L.Oligocene	-	-	-	45.1/1.25
5-10	Tuff	L.Oligocene	-	-	-	50.7/19.0
7-3	Mudstone	M.Miocene	-	-		57.4/1.67

Pyrolytic analyses of these rocks indicate that none are good source beds for petroleum, with the possible exception of the Cretaceous mudstone (Sample #TT-1-021-001) and one Upper Jurassic sandstone (Sample #S6-77-BS-DR-1-20). However, the mudstone was dredged from the continental slope in Pribilof Canyon, 500 km southeast of the Navarin basin province. The outcrops sampled by rock dredging are generally sandy units that may not be representative of finer grained possible source beds that either are exposed along the margin or lie within the subshelf basins. Also, many of these dredge samples are from exposures that crop out too far down on the continental slope to be representative of the lower sediment sections in the basins of the Navarin province.

Traps

Strata in the northern basin of the Navarin province are

folded into anticlinal structures 10-15 km across (Fig. 7); this folding may have been caused either by diapirism or by lateral compression. Only three survey lines cross the folds here, and the size and extent of the folds are unknown. The anticlines are cut by an unconformity that is overlain by a few tens of meters of flat-lying strata. High-amplitude reflection events are observed within the strata above the balded folds. Beds in the southern two basins are cut by normal faults along the flanks of the basins. Increase in the offset across these faults with depth indicates that the faults are growth structures that formed contemporaneously with basin filling.

Potential stratigraphic traps also exist within the Navarin province. For example, lower beds in the basins' fill thin toward the basement flanks of the basins and generally dip toward the axis of each basin, so that fluids migrating updip could be trapped against denser, less permeable rocks of the Mesozoic basement. In addition, the lower stratigraphic sequence in the basins is commonly overlapped discordantly by the younger overlying beds. Thus hydrocarbons moving updip along the lower beds could be contained by impermeable layers in the upper flat-lying strata.

Other potential traps for hydrocarbons in the Navarin province include drape structures, i.e., strata in the bottom of the three basins commonly are draped over blocks in the basement and this closure could form potential traps for migrating fluids from the basement complex. Some of these features are quite large -

offset on the basement blocks is commonly several thousands of meters and the blocks extend laterally more than 5-10 km.

SIGNIFICANCE OF BOTTOM SIMULATING REFLECTORS - GAS HYDRATE ZONE AND DIAGENETIC BOUNDARY

Anomalous reflectors are observed in seismic-reflection data recorded across the Bering Sea continental slope and rise in water depths of 500 to 3,000 meters. These reflectors are called Bottom Simulating Reflectors (BSR) because they mimic the bathymetric relief of the seafloor and in many places, they cut across other layered reflectors. Recent studies indicate that two types of BSRs are present and both are caused by geologic phenomena that may be important to the hydrocarbon assessment of deep-water (greater than 500 meters) areas of the Navarin basin province (Fig. 11). The shallower of the two BSRs (BSR-GH) is believed to follow the base of a gas hydrate zone and the deeper BSR (BSR-DB) is thought to follow a silica-diagenetic boundary between overlying biogenic (Opal-A) sediment and underlying crystalline (Opal-CT) indurated mudstone. The characteristics of the two BSRs are listed in Table 2.

A BSR, now named BSR-DB, was first identified in the Bering Sea by Scholl and Creager and others (Scholl and Creager, 1973) in preliminary surveys for Deep Sea Drilling Project (DSDP) sites 184 and 185 on Umnak Plateau. Scholl and Creager (1973) suggested, and Hein and others (1978) later confirmed, that the BSR-DB is related to the diagenetic alteration of silica-rich diatomaceous deposits. Scholl and Creager and others (1973) also report

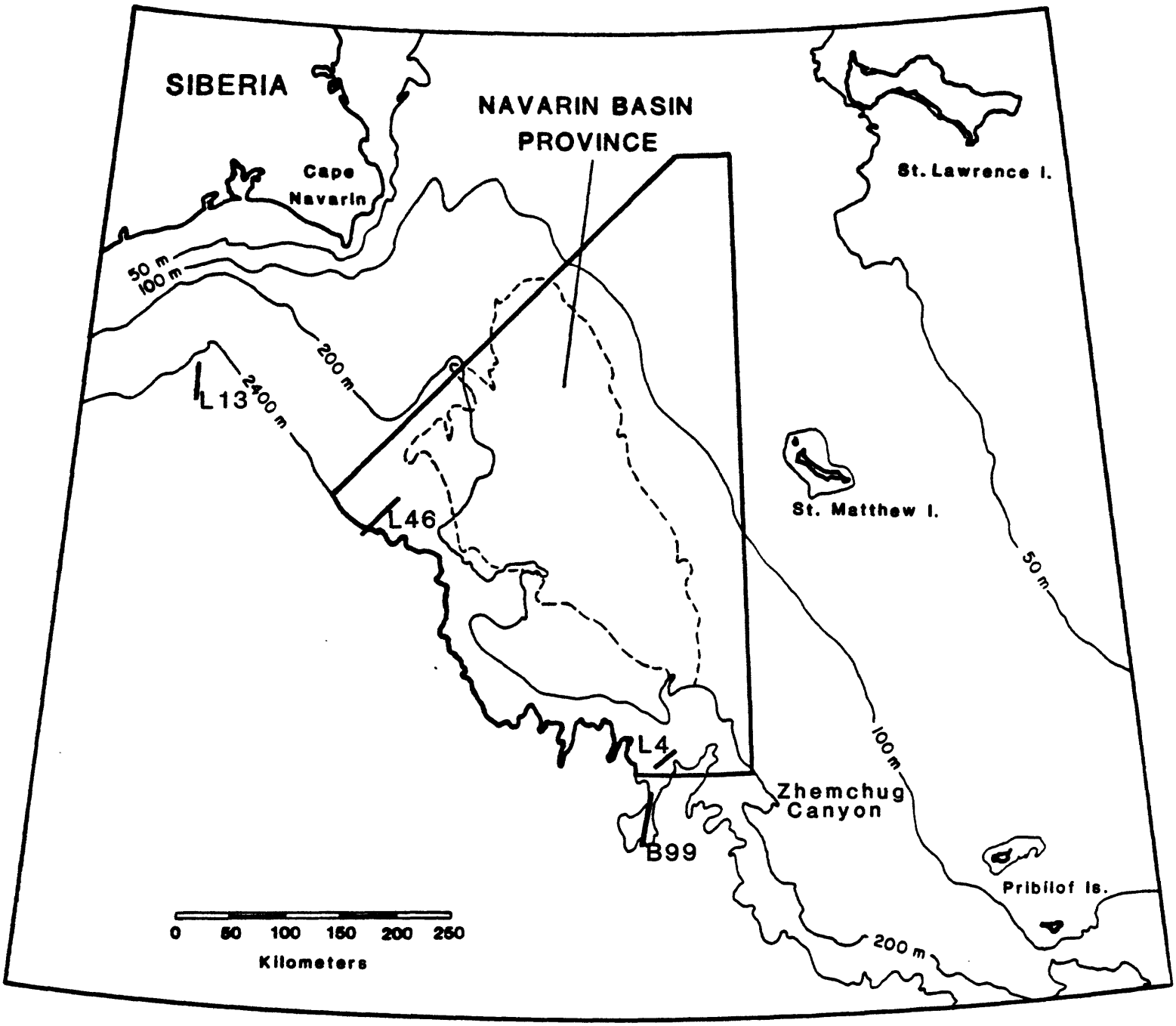

Figure 11. Location map for seismic profiles shown in figures 12 and 13.

that the prominent reflection horizon (Reflector 'P' of Ewing and others, 1965) found over Bowers Ridge (DSDP site 188) exhibits the same characteristics of a BSR-DB and is related to the alteration of diatomaceous sediment. Sonobuoy velocity studies (Cooper and others, 1979) have confirmed the initial DSDP results that a velocity increase, or velocity discontinuity, occurs at the same depth as the BSR and this discontinuity is found throughout the deep-water areas of the Bering Sea. The prominent reflection horizon, which corresponds to the velocity discontinuity, can be traced to the Bering Sea margin and again appears as a BSR-DB (Figs. 12, 13) that cuts across layered reflectors. Cenozoic rocks dredged along the margin are primarily unaltered diatomaceous mudstones (Marlow and others, 1979a) and are typical of those found above BSR at DSDP sites on Umnak Plateau. Indurated and altered rocks have not been sampled from beneath the BSR because either the BSR is buried or the sedimentary section is eroded along the sections of the margin that have been sampled.

A second and shallower BSR (BSR-GH) has been identified only recently in the Bering Sea and has geophysical characteristics different from those of the diagenetic boundary BSR (BSR-DB). The characteristics of the new BSR-GH (Table 2) are similar to those described by Shipley and others (1979) for the base of a gas hydrate zone. The initial drilling reports concerning BSR-DB on Umnak Plateau (Scholl and Creager, 1973) and the later geophysical analysis of BSR-DB by Shipley and others (1979)

TABLE 2 - BSR TYPES FOUND IN THE BERING SEA

		GH - Gas Hydrate	DB - Diagenetic Boundary
I. General			
1.	Description	Reflector that marks the base of a gas hydrate zone - the transition from gas hydrate to free gas.	Reflector that marks a silica diagenetic boundary between overlying biogenetic (Opal-A) sediment and underlying indurated crystalline (Opal-CT) mudstone.
2.	Areal distribution	Presumed regional in extent, for water depths greater than 500 m. Identifiable most easily in areas with topographic relief and undeformed sediment cover.	Regional extent throughout deep-water (>200 m) provinces of the Bering Sea, where siliceous diatomaceous sediment are found or are presumed to be present.
3.	Controlling factors	Sufficient gas concentrations; suitable pressure/temperature conditions.	Appropriate conditions (temperature, pressure, geochemistry) for diagenesis of biogenic to crystalline silica.
II. Geophysical Signature			
1.	Geometry	Reflector that mimics seafloor topography and commonly cuts across other layered sub-seafloor reflectors.	Same description as BSR-GH but usually found at greater sub-seafloor depths than BSR-GH.
2.	Sub-seafloor depth	Depth to BSR increases with increasing water depth - usually found at 200-500 m (0.3-0.6 sec) sub-seafloor.	Depth to BSR decreases or remains same with increasing water depth - usually found 700-1100 m (0.9-1.2 sec) sub-seafloor.
3.	Sub-seafloor velocity	Higher than typical sediment velocity above BSR-GH.	Higher than typical sediment velocity below BSR-DB.
4.	Phase of BSR reflector	Inverted (negative) phase for BSR-GH.	Normal (positive) phase for BSR-DB.
5.	Amplitude of of BSR reflector	Highly variable, commonly faint and hard to see. Gas hydrate zone, above BSR-GH, is associated with diffuse or faint reflectors in some areas.	Usually large amplitude and easy to see except where BSR-DB is parallel to other reflectors.

Table 2 - BSR TYPES FOUND IN THE BERING SEA (Continued)

		GH - Gas Hydrate	DB - Diagenetic Boundary
III.	Significance for Hydrocarbon Distribution		
1.	General	Gas hydrate zone may: 1) contain significant quantities of included gas, 2) act as a seal that prevents upward migration of hydrocarbons.	Diagenetic boundary: 1) has a major decrease in porosity and permeability beneath the boundary, 2) may influence migration path and trapping of hydrocarbons.
2.	Traps	Hydrocarbons (liquid? and gas) may be trapped and accumulate beneath impermeable gas hydrate zone.	In areas of bathymetric relief, laterally migrating hydrocarbons may be trapped against diagenetic boundary. Trapping beneath the boundary may occur in porous interbedded layers
3.	Migration of hydrocarbons	Lateral migration of hydrocarbons along base of gas hydrate zone.	Migration of hydrocarbons beneath the boundary is via facture porosity and permeability within unaltered sediment originally poor in biogenic silica.
4.	Operational hazards	Packets of overpressured gas may be trapped beneath gas hydrate zone.	Decollement surface along which major sediment bodies may slide and slump.

indicate that BSR-DB is not associated with significant methane gas and does not conform to the theoretical temperature-pressure relations required for a gas hydrate horizon. The existence of gas hydrates in the deep-water parts of the Bering Sea has been hypothesized by Scholl and Cooper (1978) in a study of deep-water bright spots (VAMPs) in the abyssal Aleutian Basin. Analysis of surface sediment from the Aleutian Basin and southern Bering margin (Kvenvolden and Redden, 1980) show low concentrations of gases in the upper 1-2 meters beneath the seafloor. The low concentrations imply that hydrates, if present at depth, do not exist immediately beneath the seafloor. However, along the northern and central areas of the margin, where the BSR-GH is most common, the presence or absence of hydrates has not been confirmed by sub-seafloor sampling.

Seismic-reflection records collected near the Navarin basin province (Fig. 11) show that a few deep-water areas of the slope and rise contain both BSR-GH and BSR-DB. Three seismic profiles (L46, L4, B99; Figs. 12 and 13) show the simultaneous occurrence of both BSRs. Since BSR-GH is often a weak reflector (L46, Fig. 13) it is difficult to identify except in those areas that have bathymetric relief and an undeformed sediment cover. In contrast, BSR-DB, is a strong reflector and is usually seen in those areas that have sufficient (700 to 1,100 meters) sediment cover for diagenesis of biogenic to crystalline silica.

The geologic phenomena that create the two BSRs may be important to future hydrocarbon exploration in the slope and rise

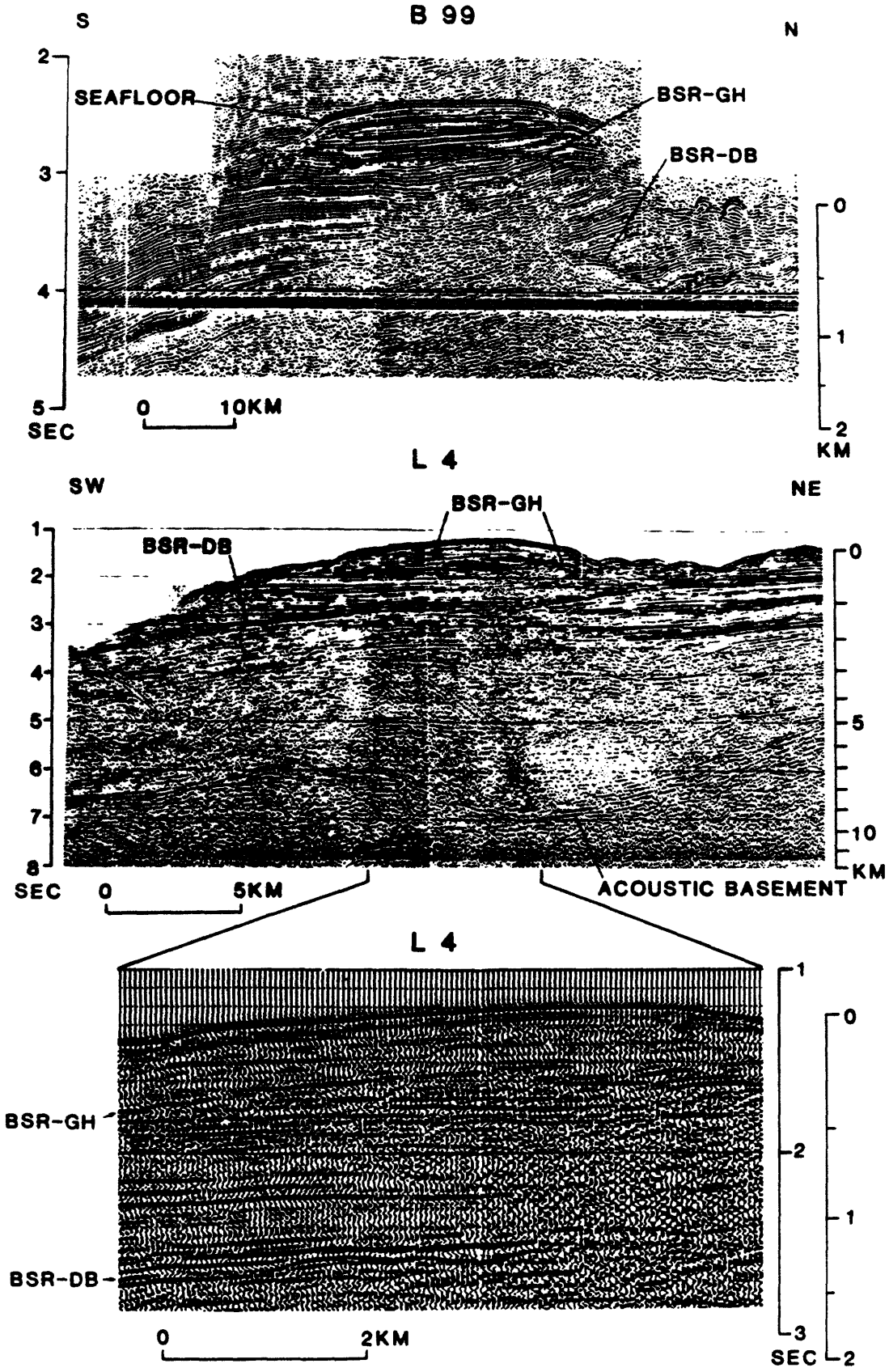

Figure 12. Seismic profiles B99 and L4 collected along the slope areas of the Navarin Basin province. The profiles show two BSRs, one at the base of a gas hydrate zone (BSR-GH) and one at a silica-diagenetic boundary (BSR-DB). See figure 11 for location.

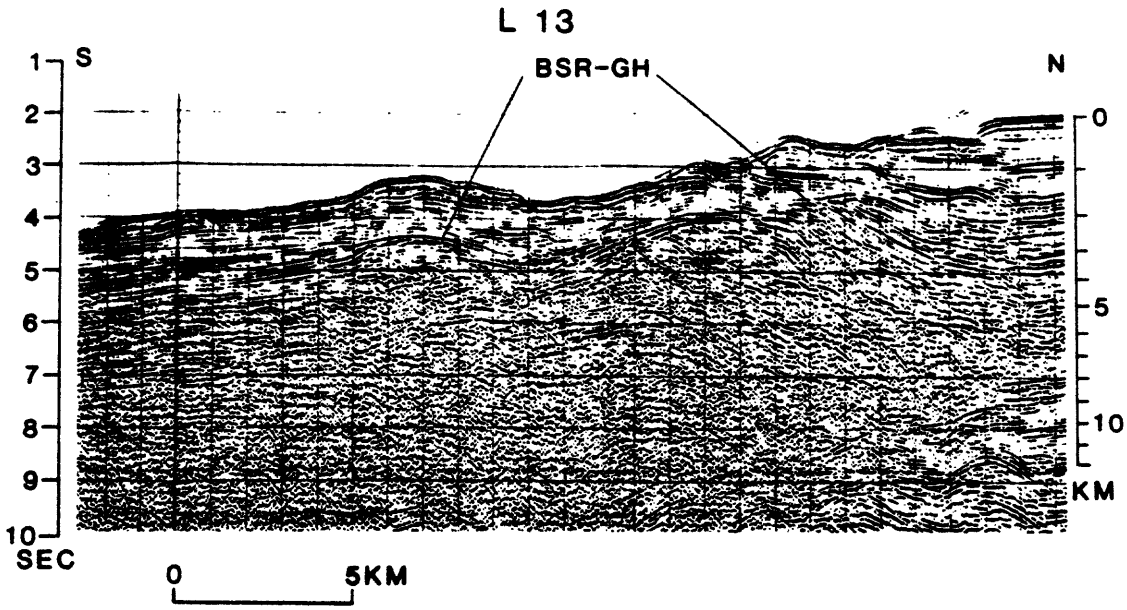

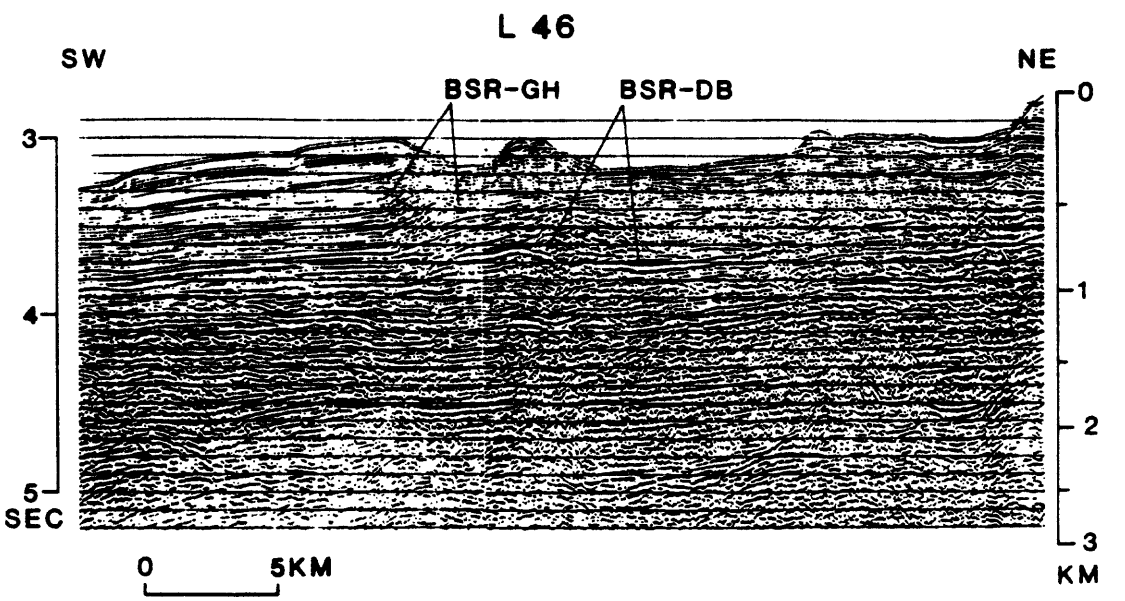

Figure 13. Seismic profiles L13 and L46 collected along the slope areas in and around the Navarin Basin province. The profiles show two BSRs, one at the base of a gas hydrate zone (BSR-GH) and one at a silica-diagenetic boundary (BSR-DB). See figure 11 for location.

areas and the reasons for their significance are outlined in Table 2. The gas hydrate zone (whose base is marked by BSR-GH) may contain significant quantities of natural gases and the zone may act as an impermeable barrier to the upward migration of other liquid or gas hydrocarbons that are trapped beneath the hydrate zone. Similarly, the diagenetic boundary (BSR-DB) may be an important controlling factor in the migration path, trapping, and sealing of migrating hydrocarbons.

The widespread distribution of both types of BSRs indicates that if hydrocarbons are present beneath the slope and rise, the diagenetic boundary and gas hydrate zone may be important factors in locating hydrocarbon accumulations.

SEAFLOOR GEOLOGIC HAZARDS

Potential geologic hazards in the Navarin basin province include faulting and earthquakes, seafloor instability due to submarine landslides, sediment transport and erosion, and subsidence or blow-outs resulting from disturbance of gas-charged sediment, volcanic activity, and ice. Seafloor instability probably poses the greatest seafloor hazard. Because there has been only one cruise to Navarin basin that was devoted solely to the collection of geohazard data, and that was in July-August 1980, all of the following interpretations must be considered preliminary. Another cruise is planned for the summer of 1981, when additional geohazard data will be collected.

Faulting and Seismicity

The limited seismic coverage in the Navarin basin province

restricts the interpretation of faults with respect to their length, orientation, and age. The distribution of the faults is shown in Figure 14; however, the wide spacing of the tracklines (about 30 km) makes correlation from line to line extremely tentative. The faults located on lines oriented perpendicular to the long axis of Navarin basin greatly outnumber those on lines that parallel the axis of the basin, suggesting a northwest-southeast trend of the faults. This trend is parallel to the basin axis and to the shelf-slope break. The majority of these faults occur on the continental slope and outermost shelf.

The faults may or may not show offset of the acoustic basement. Many of the faults shown on Figure 14 are mapped from high-resolution seismic-reflection records that have resolution of 1-3 meters of the seafloor; however, none of the faults mapped to date show offset of the Holocene seafloor.

Although the ages of the faults are unknown, C_{14} dates of sediment in the southern part of the area indicate accumulation rates of the upper 6 meters of sediment to be about 25.0 $cm/10^3 yrs$ (Askren, 1972). Therefore, faults that reach to within 3 meters of the seafloor may cut sediment as young as 12,000 yrs. B.P. and must be considered active.

According to Scholl and others (1975), Cooper and others (1976c), and Marlow and others (1976), subduction of the Kula plate beneath the Bering Sea margin apparently ceased in late Mesozoic or early Tertiary time and subduction of the Pacific plate shifted to near the present Aleutian Trench. This transfer

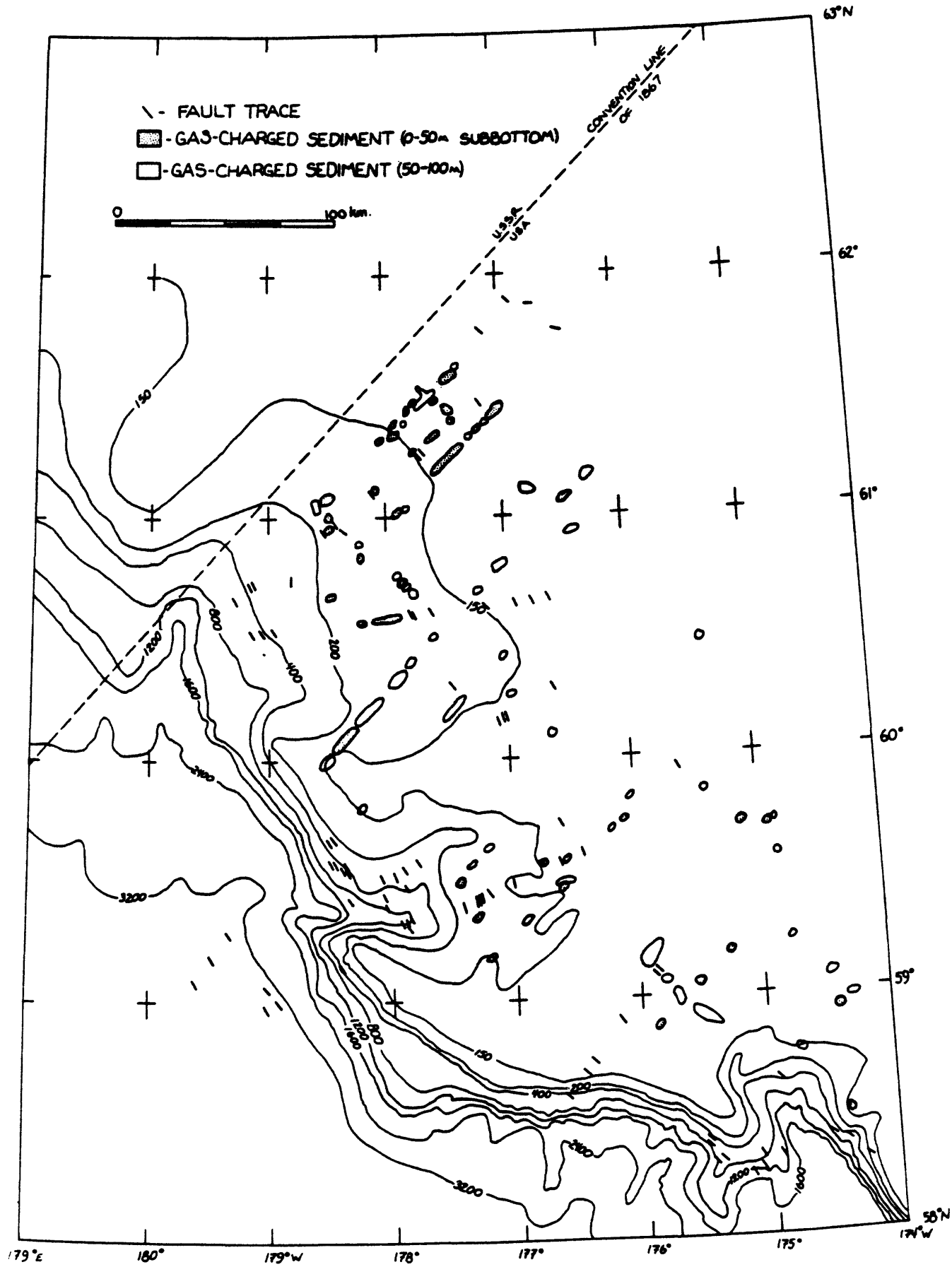

Figure 14. Preliminary map of fault traces and areas of gas-charged sediment in Navarin basin province. Lines of fault trace are drawn at right angles to line of seismic profiles. Bathymetry in meters.

apparently tectonically deactivated the Bering Sea margin. The lack of modern seismicity is readily seen on the maps of Alaska earthquake epicenters published by Meyers (1976). Only six earthquakes have been reported from the Navarin basin province for the time period prior to 1974, and all were less than magnitude 6 earthquakes. These data may be somewhat misleading because of the wide spacing and limited number of seismograph stations in western Alaska. In order to determine the occurrence of low-magnitude earthquakes in a place as remote as Navarin basin, the emplacement of a group of ocean-bottom seismographs is necessary.

Seafloor Instability

Within the broad category of seafloor instability, we have included discussions of three major types: submarine landslides, sediment transport and erosion, and gas-charged sediment.

Submarine Landslides

Submarine landslide is used as an all-inclusive term for a variety of slope movements. The preliminary nature of our study makes it impractical at this time to attempt to classify each of the areas of slope movement according to type of movement and type of material. As we progress with the study, we shall be able to describe and delineate the landslides more completely, and we will attempt to sample within and adjacent to the slides in order to determine the composition of the sediment and its geotechnical properties.

The continental margin of the Navarin basin province is incised by three large submarine canyons that are associated with many of the submarine slides mapped thus far (Fig. 15). None of the slides begins in water shallower than 200 m, several begin below 400 m, and one appears to begin at a depth of greater than 1,200 m. In five areas of the continental slope, the length of the zone affected by slope movement is at least 50 km. Because of the preliminary nature of the data, the exact delineation of these slide masses has not been determined; however, some of these zones appear to be 25 km wide. The landslides may affect the upper 200-300 m of the sediment column. Gravity cores (2-5 m) were collected from a few of the slide masses. These cores varied in sediment types from pebbly mud to sandy mud to very soft oversaturated mud. Additional sampling is needed to accurately delineate the physical properties of the slide masses.

Preliminary evaluation of the seismic profiles crossing the outer continental shelf and slope suggests that the slope movements can be described according to Varnes' (1978) classification as ranging from slumps to debris slides to earth flows. The most likely triggering mechanisms of the submarine landslides are agitation of the underconsolidated sediments by storm waves, internal waves, or tsunamis. Less likely causes of sliding in this region are prolonged ground shaking during earthquakes, overloading and excessive steepening by erosion and/or rapid sediment accumulation, and buildup of excessive pore-water pressures in underconsolidated clayey sediments due to

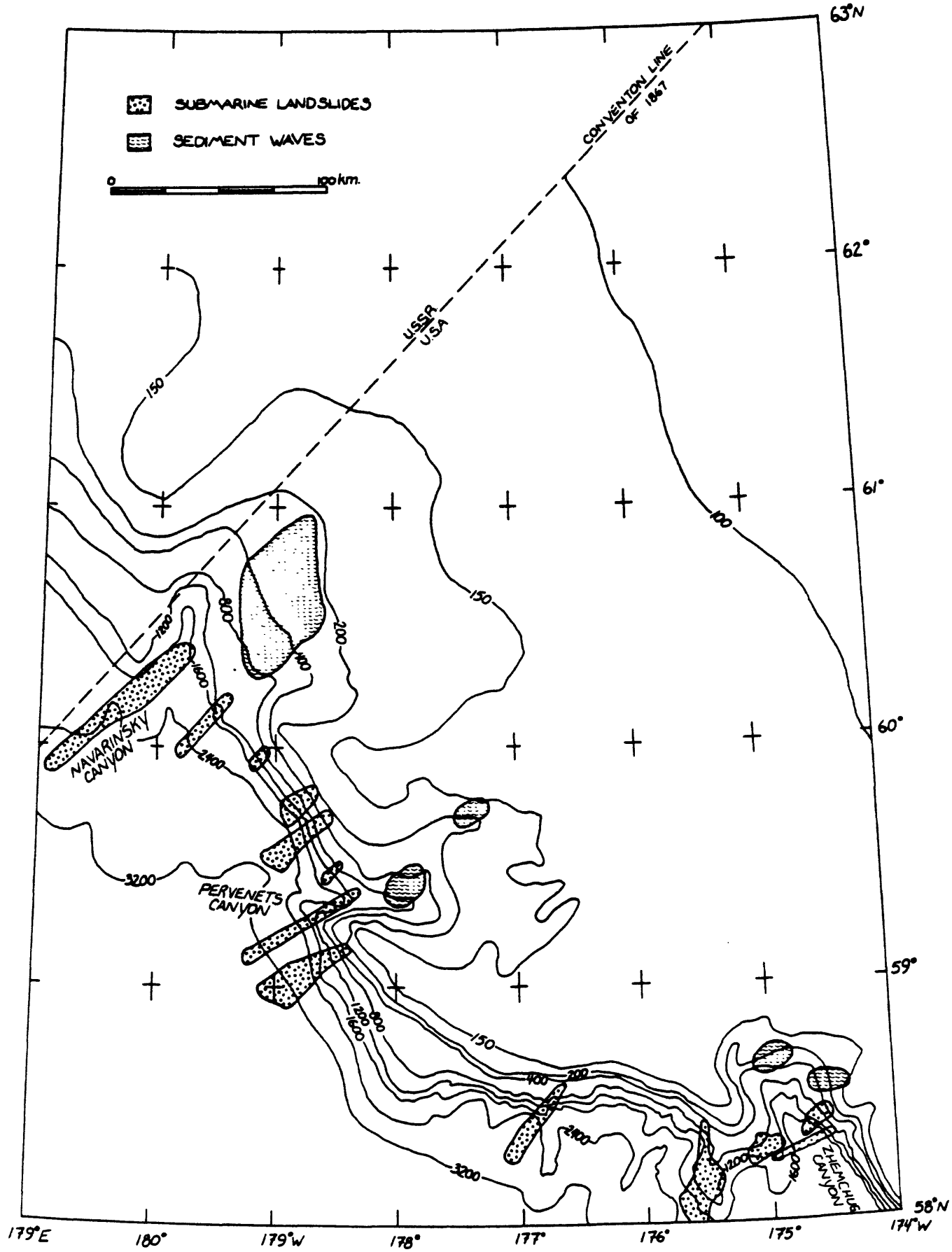

Figure 15. Preliminary map of identified areas of submarine landslides and sediment waves in Navarin basin province. Bathymetry in meters.

rapid sedimentation or increasing concentrations of gas in the sediment.

Sediment Transport and Erosion

Sediment Types.

Until now we have been able to perform laboratory grain-size analyses on only a few of the more than 100 cores and grabs collected during summer 1980. Figure 16 is a preliminary map derived from visual examinations of surface samples conducted onboard ship. We have listed mean grain diameter at those stations for which samples have been analyzed.

Most of the surficial sedimentary cover consists of olive gray, greenish gray, to grayish olive green silt to silty sand. Although many of the cores show a uniform lithology, some cores or sections of cores show lithologic changes or contain exotic clasts or sand and silt "turbidite" layers.

We can discern two tentative trends from the preliminary data set. Whereas silts generally characterize the shelf and slope, there seems to be a zone of coarser sediment at the shelf break, on the upper slope, and in the heads of the submarine canyons. Also, surficial sediment cover on the shelf seems to be slightly coarser in the southeastern part of the lease area than elsewhere. More detailed descriptions and interpretations are dependent upon the completion of grain-size analyses in progress.

Large Bedforms.

Large sediment waves have been observed at the heads of

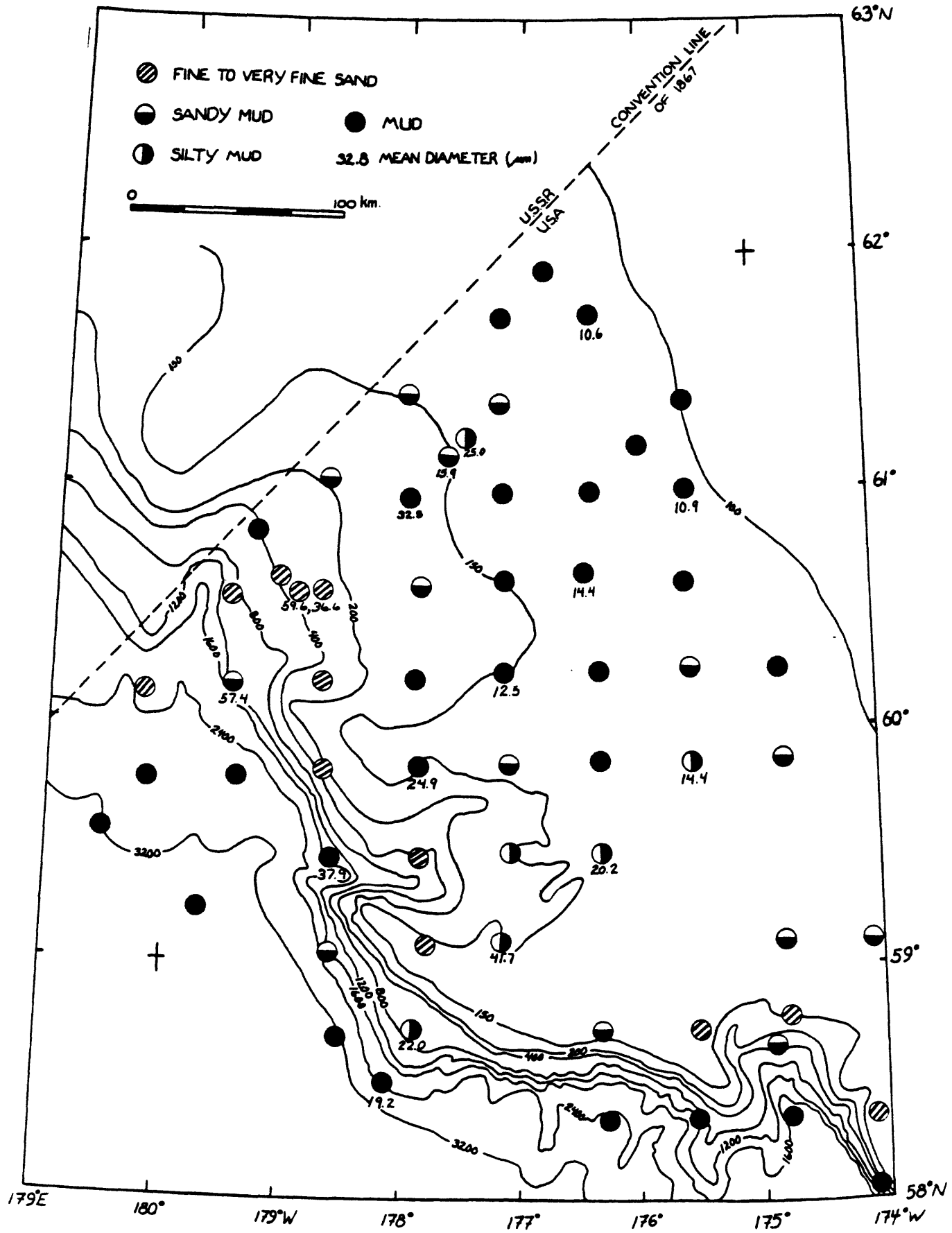

Figure 16. Preliminary map of sediment types in Navarin basin province derived from visual inspection of core samples onboard ship. Mean grain diameter (μm) listed at those stations for which samples have been analyzed. Bathymetry in meters.

Zhemchug, Pervenets, and Navarinsky submarine canyons (Fig. 15). The sediment waves in each area are similar. Those at the head of Navarinsky canyon have been studied in greatest detail. They occur on a substrate of silty very fine sand within a 600-700-km^2 area between the 215- and 450-m isobaths. These bedforms strike approximately north-south, have an average wavelength of about 600 m, and have an average height of about 8 m and a maximum of about 15 m. Both symmetrical and asymmetrical waves have been observed. The bedforms are not only expressed on the surface, but also are remarkably well defined in the subsurface. The stratigraphic unit containing the sediment waves has developed over a flat-lying reflector and attains a maximum thickness of about 120 m in the sediment wave field.

We can only speculate on the origin of these bedforms at this stage of our investigation. We do not know if they are relict or presently active, nor are we certain if they indicate continuous sedimentation or discrete episodes of activity and non-activity. If these features are active, they, as well as the processes responsible for them, could represent seafloor hazards. The hydrodynamic interpretion of these sediment waves, however, requires more detailed analysis of existing data and further field investigation.

Surface Waves.

Currents generated by surface waves probably are a more significant factor in the transport of silt and larger size particles on the open slope and shelf of Navarin basin than, for

example, tidal currents or the mean circulation. Bottom currents have not been measured in the lease sale area, nor are there good observations of surface waves. However, some surface wave data has been compiled in areas adjacent to and including a portion of the eastern boundary of the lease sale area (Brower and others, 1977).

Storms, and consequently storm-generated waves, are strongest and most frequent during the fall and winter (Lisitsyn, 1966; Brower and others, 1977). Waves as high as 15 m with possible periods of 9-11 seconds have been observed just to the east of the lease area (Brower and others, 1977). Whereas waves of such great heights are hazardous to ships or structures at the water surface, they do not generate currents of sufficient strength near the seafloor to erode sediments over a large portion of the shelf within the lease area. Assuming a threshold value of 10 cm/sec for fine sand (Komar and others, 1972), a 15-m-high, 11-second-period wave generates currents strong enough to erode fine sand only in water shallower than 125 m. A wave 10 m high with a 15-second period, however, produces near-bottom currents greater than 10 cm/sec in water as deep as 200 m. These data indicate that storm waves are a potential hazard in the Navarin basin area.

Gas-Charged Sediment

Gas-charged sediment has reduced strength and bearing capacity as compared to the strength of gas-free sediment. As the gas concentration increases, excess pore pressure increases

and sediment stability decreases until failure occurs. Failure of the sediment poses a potential hazard to seafloor exploitation because drilling into gas-charged sediment, disruption of the sediment by cyclic loading, or spontaneous over-pressurization may cause a sudden release of gas leading to failure of pipelines or platforms.

The numerous areas of gas-charged sediment mapped in the Navarin basin province (Fig. 14) are identified on the high-resolution seismic-reflection profiles by acoustic anomalies such as displaced reflectors and "wipe-out" zones. These anomalies are prevalent in the upper 50 to 100 m of sediment. Many of these shallow anomalies coincide closely with well-developed "bright spots" that show up deeper in the section on multichannel or medium-resolution single-channel profiles.

Gravity cores collected throughout the province in the summer of 1980 were analyzed for hydrocarbons (methane through butanes). All of the cores sampled contained hydrocarbon gases, but none showed significant amounts of thermogenic hydrocarbons. Three cores, two from the shelf and one from the slope, contained concentrations of methane and ethane 5-9 and 10-20 times, respectively, higher than background values (Vogel and others, 1981). These cores also contained ratios of ethane to ethene and methane to ethane and propane that marginally suggest the presence of some thermogenic hydrocarbons. A possible explanation for the low concentrations of hydrocarbons is the short length of the cores.

Volcanic Activity

Although no evidence of active volcanism exists in the Navarin basin province, the volcanically active Alaska Peninsula and Aleutian Islands mark the southern border of the Bering Sea. Coats (1950) lists 25 active volcanoes in the Aleutian Islands and 11 on the Alaska Peninsula. Volcanism on the Pribilof Islands, less than 500 km southeast of Navarin basin, is very recent. Volcanic hazards are associated with eruption of lava and ash and the accompanying earthquakes.

Eruptions from large andesitic cones like those found on the Aleutians and the Alaska Peninsula are explosive and can spread pyroclastic material over large areas. Eruptions from basaltic volcanoes like those on the Pribilof Islands are less explosive and would have local effects.

About 21 km^3 of ash was erupted in Alaska in 1912 by Katmai volcano when ash was carried over distances of 2,000 km or more. At a distance of 180 km from the volcano, ash was deposited with a density of about 45 g/cm (Lisitsyn, 1966). According to historical data, individual ash deposits in the Bering Sea region extend 200 to 2,000 km from the source, averaging about 500 km.

Ice

We have estimated ice conditions in the Navarin basin province by synthesizing data reported in Lisitsyn (1966), McRoy and Goering (1974), and Brower and others (1977). The proposed lease area is ice-free from June through October. Migratory pack

ice begins to encroach upon the northern part of the lease area in November. The pack ice is fully developed by March or April at which time the extreme southern limit of the ice edge extends over most of the lease area. Ice concentrations begin to decrease in April and the ice edge continues to retreat northward through May. First-year ice in the southern portion of the Bering Sea ranges in thickness from 30 to 71 cm, whereas ice further north can attain a thickness of 1-2 m in unstressed floes. The southern limit and concentration of the pack ice varies from year to year depending upon weather conditions--some years migratory pack ice may not affect the lease area, but in other years concentrations of ice may completely cover it.

RANKING OF AREAS CONSIDERED PROSPECTIVE FOR HYDROCARBON DEPOSITS

Figure 17 outlines the area being considered for lease in the northern Bering Sea. Within this area we have ranked three subregions as to their probability of containing hydrocarbon deposits. The region with the greatest chance for hydrocarbon accumulations is the zone underlain by the three Navarin basins (>2 km sediment thickness, Fig. 17). As outlined in previous sections of this report, the Navarin basin province contains thick (>12 km) sedimentary sections that are broken by high-angle normal faults flanking the basin. Offset along these faults increases with depth, indicating that they are growth structures and possible traps for hydrocarbons. Regional geologic studies indicate that suitable source and reservoir rocks are probably

present within the Navarin basin province.

The area of secondary ranking is that area in the province that is underlain by sedimentary sections 1-2 km thick. The areas considered to have the least potential are also outlined in Figure 17. These areas in the province are underlain by a sedimentary section less than 1 kilometer thick, probably too thin for the generation of hydrocarbons, at least in the section overlying acoustic basement. Thus, any exploration targets would have to be structures within the basement complex beneath this part of the province. Size, extent, and existence of such features is unknown and hence the low ranking of these areas.

HYDROCARBON RESOURCE APPRAISAL

The area considered in this appraisal is bounded on the north by 63°N latitude, on the northwest by the U.S.-Russia convention line of 1867, on the east by the 174°W meridian, on the south by 58°N latitude, and on the southwest by the 2,400-meter bathymetric contour. This total area has been divided by the 200-meter bathymetric contour and separate assessments prepared for the Navarin shelf and Navarin slope. The estimates are assessments of undiscovered recoverable oil and gas. These quantities are considered recoverable at current cost and price relationships and at current technology, assuming additional short-term technological growth.

The assessments are probability estimates of "more than" quantities associated with given probabilities of occurrence. The estimates are stated two ways. First, the conditional

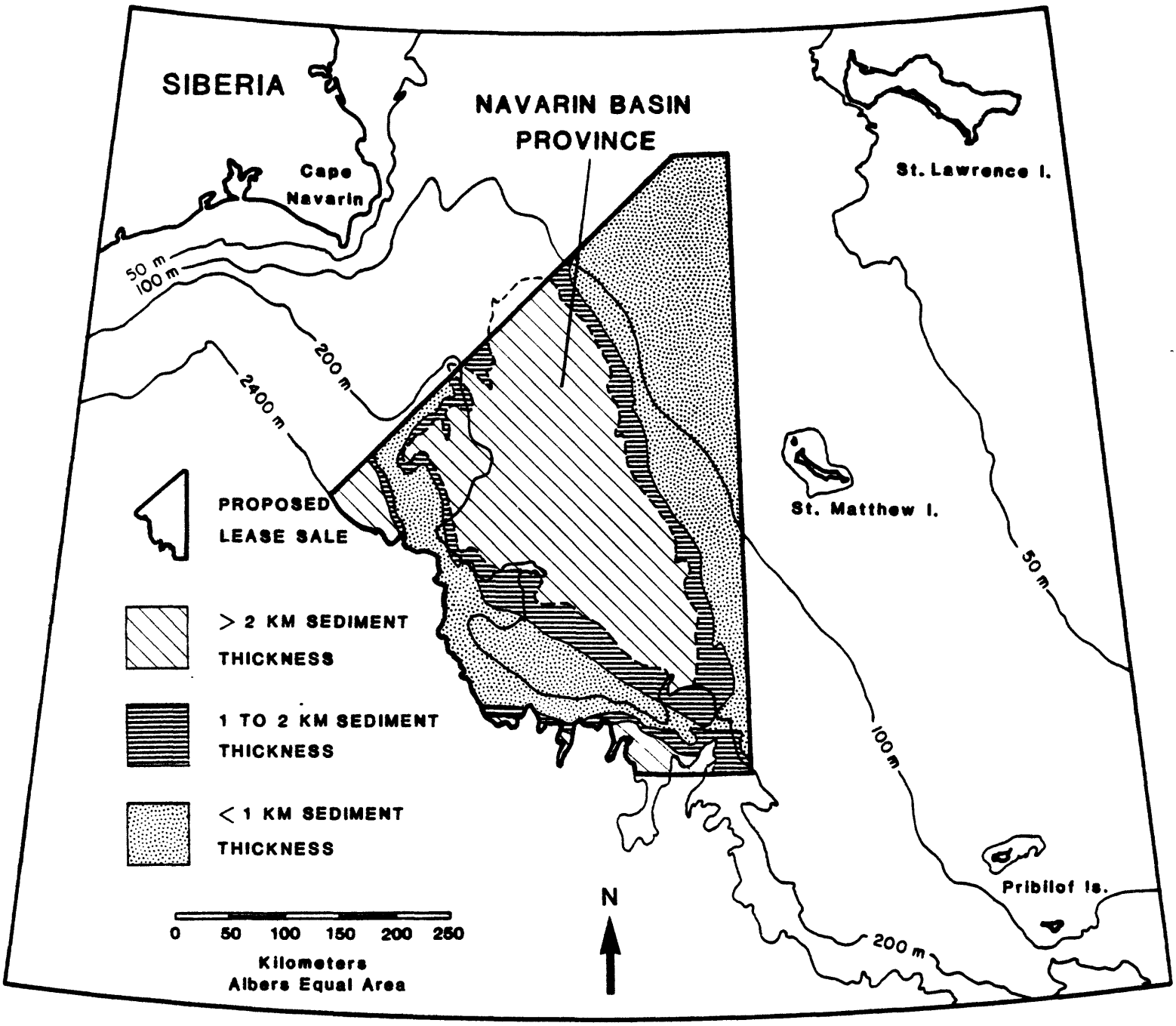

Figure 17. Outline of proposed OCS Lease Sale #83 (Navarin basin province) and generalized isopach map of sediment thickness above "acoustic basement". Based in part on Figure 8. Areas with sediment thickness greater than 2 kilometers are considered most prospective for hydrocarbon accumulations. Albers equal area projection.

estimates are those quantities that may be present assuming that commercial quantities do exist. Second, the unconditional estimates are those quantities that may be present when the probability that no commercial hydrocarbons exist is included. The probability of finding commercial quantities in frontier areas such as the Navarin basin province is uncertain. A marginal probability is used to express this risk and estimates of this marginal probability are made for each set of conditional estimates. The marginal probability and conditional estimates are used to calculate the unconditional values.

Estimates of the undiscovered oil and gas resources for the Navarin shelf (0-200 m) are shown in Table 3 and for the Navarin slope (200-2400 m) in Table 4. The aggregated total gas estimates include associated-dissolved gas and non-associated gas. Three possibilities exist for the occurrence of the gas resources. A basin might contain both associated-dissolved gas and non-associated gas, only non-associated gas, or only associated/dissolved gas. All three cases are included in the estimates for total aggregated gas in Tables 3 and 4.

Subjective probability techniques were used to produce the basin assessments and they incorporate geologic judgments and analyses of the petroleum characteristics of the basin. The analytical procedures include:

1. A review and interpretation of available geological and geophysical data.
2. Application of arbitrary hydrocarbon yields derived from

various United States hydrocarbon-producing basins.

3. Comparison with other petroleum provinces.

Regional geology and geophysical data suggest that sufficient sedimentary thickness is present in the Navarin basin for the generation of hydrocarbons. Suitable structural and stratigraphic traps for hydrocarbons are also indicated by seismic-reflection data. However, the existence and maturation of source beds as well as the presence of adequate reservoir beds are largely unknown. These unknown factors are the principal risks in finding commercially recoverable hydrocarbons in the Navarin basin. The Navarin basin may be analogous to Bristol Bay basin and the St. George basin in the Bering Sea shelf and the Anadyr basin in eastern Siberia. Soviet wells in the Anadyr basin have recovered natural gas and condensate but not in commercial quantities.

Table 3. Estimates of Total Undiscovered Recoverable Oil and Gas, Navarin Shelf (0-200m)

	95% Probability	5% Probability	Statistical Mean	Marginal Probability
Oil (billions of barrels)				
Conditional	.17	6.45	1.87	.41
Unconditional	0	3.66	.77	--
Assoc./dissolved Gas (TCF*)				
Conditional	.26	9.67	2.81	.41
Unconditional	0	5.51	1.15	--
Non-assoc. Gas (TCF*)				
Conditional	1.98	23.11	8.79	.45
Unconditional	0	16.61	3.96	--
Aggregated Gas (TCF*)				
Conditional	.40	22.58	7.51	.68
Unconditional	0	19.63	5.11	--

* TCF, trillion cubic feet

Table 4. Estimates of Total Undiscovered Recoverable Oil and Gas, Navarin Shelf (200-2400m)

	95% Probability	5% Probability	Statistical Mean	Marginal Probability
Oil (billions of barrels)				
Conditional	.21	1.45	.60	.16
Unconditional	0	.63	.10	--
Assoc./dissolved Gas (TCF*)				
Conditional	.32	2.17	.90	.16
Unconditional	0	.95	.14	--
Non-assoc. Gas (TCF*)				
Conditional	.90	3.40	1.67	.19
Unconditional	0	1.85	.32	--
Aggregated Gas (TCF*)				
Conditional	.40	3.34	1.44	.32
Unconditional	0	2.23	.46	--

* TCF, trillion cubic feet

OPERATIONAL CONSIDERATIONS

Technology, Infrastructure, and Time Frame

Estimation of development times in Navarin Basin, an Alaskan offshore frontier area, is a difficult matter. Although the latitude is about the same as the northern oil fields of the North Sea, the weather of the Bering Sea is more severe than that of the North Sea. It is colder than the North Sea and is covered with moving sea ice several months of the year. Navarin Basin is also much further from industrial support bases and population centers. The adverse weather, severe sea conditions and very great distances from supply bases and established transportation and market infrastructure will cause delays in operations and increased costs.

Exploratory drilling will probably commence within 2 years

after the lease sale. Assuming exploratory success, production platform installation would begin during the fifth or sixth year after the leases are issued and developmental drilling should be completed by the fifteenth year. Subsea completions and offshore loading and storage facilities may be included in this development phase.

Peak oil production, if not limited by marketing facilities, would occur about the eighth year after the lease sale. Individual fields would have a 25-year life, and all production activities will have ceased by the fortieth year after production begins.

It is estimated that the smallest fields that can be economically developed in this area will have to contain about 50 million barrels of recoverable oil, or about one trillion cubic feet of gas in non-associated dry gas fields. However, the rapidly escalating price of hydrocarbons and the feasibility of economical ship transport to the U.S. West Coast may justify the development of even smaller fields, especially if marketable hydrocarbons are found in other Bering Sea basins such as St. George, Norton Sound, or the Northern Aleutian shelf.

For estimating the number of fields, the average reservoir is assumed to be 2.5 times the size of the minimum economic field, and the largest single reservoir is assumed to be 10 times the size of the minimum.

Assuming 10 million barrels recovery per well, 40 wells maximum per production platform would give the following figures

for the number of wells and daily production of oil and gas for the conditional, or unrisked, minimum and most likely cases:

	95% Probability	5% Probability	Statistical Mean
Recoverable oil BBbl*	0.17	6.45	1.87
Oil Fields	3	45	16
Wells (including service)	26	968	281
Peak production MBbl/day*	54	2032	589
Gas-oil ratio	1500	1500	1500
Peak gas production MM cu. ft/day*	80	3048	884

* (B = billion, M = thousand)

The number of service wells is based on experience in the North Sea where there are about half as many service wells as there are production wells. The above production figures are based on producing 11.5 percent of the recoverable reserves in the peak year.

Assuming that a non-associated gas field in this area must contain about one trillion cubic feet of gas to be economically viable for a 20-year life of constant-level production, the conditional, or unrisked parameters would be as follows:

	95% Probability	5% Probability	Statistical Mean
Gas TCF*	1.98	23.11	8.79
Gas Fields	2	8	6
Gas MMCFD	271	3165	1204
Gas Wells	20	231	88

* (T = trillion, MM=million)

Number of gas wells required and daily production figures are based on average North Sea production experience.

In case gas not associated with oil is found near oil-associated gas (gas cap and dissolved gas), it may be economical to use the same pipelines to transport the gas to shipping facilities. During the early years of oil production, associated and nearby non-associated gas is often injected into the oil reservoir to increase oil recovery.

Estimated Facilities

There are no close places suitable for exploration bases for Navarin basin. The two closest points of land are St. Matthew Island and Cape Navarin, and each is about 280 kilometers (175 miles) from the center of the Navarin basin. St. Matthew Island is taken up entirely with the Bering Sea National Wildlife Refuge and has no towns, people, airfields, or harbor facilities. Cape Navarin is in the USSR.

Gambell and Savoonga, two native villages on St. Lawrence Island, are about 360 kilometers (225 miles) from the Navarin basin, have small airfields and weekly air service from Nome, but have no harbor or dock facilities.

The next closest places are Nome, on the Seward Peninsula, and St. Paul on the Pribilof Islands, both about 644 kilometers (400 miles) from the Navarin basin. Both places have small airfields and scheduled air service, but no harbor facilities. St. Paul is a very small community and would require a considerable buildup of facilities to serve as an exploration base.

Adak and Dutch Harbor are both about 1130 kilometers (700 miles) from the Navarin basin, have airfields, scheduled air

service, and harbor facilities. However, Adak is entirely a U.S. Naval Station and Dutch Harbor is a busy fishing port with little room or facilities to spare for petroleum exploration support.

Kodiak is the nearest significant port with adequate harbor, dock, airport, and support facilities. It is about 2090 kilometers (1300 miles) by water from the Navarin basin via Unimak Pass.

Seattle is about 4350 kilometers (2700 miles) southeast of the Navarin basin, and Yokohoma is about 4500 kilometers (2800 miles) to the southwest. All of the pipe, mud and other supplies and equipment must be brought from the lower 48 states or perhaps from Japan.

For exploration of the Navarin basin, the most practical method of support may be to load everything needed aboard a large ship and keep it near the drill rigs.

Technology for successful drilling in northern offshore climates has been exhibited in Cook Inlet and the North Sea. Large semisubmersibles have been successfully used for drilling in such harsh environments. The water depth in the Navarin basin is generally beyond the limit for jack-up rigs and is also too deep for artificial gravel islands. The water depth over the most prospective parts of the basin is about 100 meters (330 feet). Large drillships may also be used. In the event that drilling is conducted year round, drillships or semisubmersibles equipped to be quickly disconnected from the well when threatened by floating sea ice would be the favored equipment. Strengthened

drill rigs and icebreaker assistance would also be of value in extending the drilling season.

Production platforms, engineered to withstand floating sea ice, would be used. In Cook Inlet, several steel platforms including a monopod platform have been used successfully for some years in the high tidal, strong wind, and floating ice environment of Cook Inlet. The ice forces to be encountered in the Bering Sea are thought to be considerably greater than those of Cook Inlet. A monopod structure that has a deflection cone positioned at the sea surface has been proposed for use in the Beaufort Sea to withstand the moving polar ice pack. The cone would cause the ice to be deflected by tension bending rather than allowing the ice to crush against the platform. Platforms would probably be constructed on the U.S. West Coast or in Japan, and towed or transported by barge to the Bering Sea.

The route to market for Navarin basin hydrocarbons will probably be via tanker to the U.S. West Coast. One of the possible places for a processing and shipping terminal is St. Paul Island in the Pribilof Islands where oil and gas would be piped ashore. Subsea completions would be advantageous because of the shifting sea ice.

Another scenario would be many subsea completions with gathering lines leading to a processing and loading terminal mounted on a steel platform that was attached to the seafloor. Storage tanks of concrete or steel resting on the sea floor could be used to store oil when no ships were present for loading. The

platform would have minimal structural members extending through the sea surface in order to offer the least resistance to the sea ice. Icebreakers could also be used during winter and spring months. In view of the cost of the many miles of pipe required to reach shore from the Navarin basin, a loading terminal at sea may be the most economical plan. An LNG (liquid natural gas) plant could be constructed in the same way if enough gas is discovered. Dome Oil of Canada has proposed a system of ice-breaking tankers for use in the Beaufort Sea as being more economical than pipelines to shore.

Seasonal production has been mentioned as a possibility for the Navarin basin. This would be one way of coping with the floating sea ice problem. Completed well heads would be on the sea floor, and production would only take place in ice-free months when there were ships to take on the oil.

In the event of major hydrocarbon discoveries in the St. George basin, Norton Sound, or the Northern Aleutian basin, all of which are scheduled to be explored before the Navarin basin, processing and shipping facilities could be combined for financial advantage.

Manpower and Drilling Equipment Availability

Approximately 80 percent of the exploration manpower would come from outside Alaska. For production, approximately 80 percent of the workers would come from personnel already in Alaska.

It is expected that there will be enough large semisubmersibles and drillships available after the sale occurs. Drilling supplies, pipe, mud, etc., should be in adequate supply.

Weather

The weather of the Bering Sea is cold, windy, and wet. A quote from the United States Coast Pilot 9 describes the weather as follows:

> "The weather over the Bering Sea is generally bad and very changeable. Good weather is the exception, and it does not last long when it does occur. Wind shifts are both frequent and rapid. The summer season has much fog and considerable rain. In early winter, the gales increase, the fogs lessen, and snow is likely any time after mid-September. Winter is the time of almost continuous storminess. Heavy winds from any direction are usually accompanied by precipitation."

There is very little weather information available about the Navarin basin area. There are no weather reporting stations nearby, and very few ships ever pass through it. The best that can be done is to look at the sketchy data available from the nearest reporting station, the Eskimo village of Gambell, on the northwest corner of St. Lawrence Island, 360 kilometers (225 miles) northeast of the Navarin Basin. Mean monthly temperatures at Gambell range from -16.2° C (2.8° F) in January to 9.6° C (49.3° F) in August. Extremes of -33.3° C (-28° F) have been

recorded in March and 21.7° C (71° F) in July. Relatively humidity is high, usually 80 to 90 percent or more. At least a trace of precipitation occurs on 275 to 300 days a year, yet the annual total is only about 37.5 centimeters (15 inches), about half of which falls during July to October. Snowfall is 60 to 75 centimeters (2 to 2.5 feet) annually. Winter winds average 32 kilometers (20 miles) per hour with recorded peak velocity of 129 kilometers (80 miles) per hour. Summer winds average 19 kilometers (12 miles) per hour with a mean maximum of 65 kilometers (40 miles) per hour. Overcast skies prevail most of the year. Clear skies are seldom seen more than 2 or 3 days a month.

Annual sea ice extends over the Navarin basin from about the middle of November to about the middle of May. The southern edge of the ice lies on a line a bit south of the Pribilof Islands extending in an arc to the southern end of the Kamchatka Peninsula during most years. It is estimated that the ice attains a thickness of about one meter (3.3 feet) with somewhat greater thickness when floes are pushed up onto each other. At Gambell, on St. Lawrence Island, average freezeup is November 21, and average ice breakup occurs May 26. The earliest freeze-up has been October 15, and the latest breakup has been July 1.

The average tidal range at St. Matthew Island is 0.64 meters (2.1 feet). Wave-height data for the area is sketchy. Judging from nearby areas, it is estimated that maximum storm wave heights may exceed 11 meters (36 feet). When the sea is ice

covered, waves are not a problem. Storm surges may cause ice movements that may endanger man-made structures. On page 438, the Bering Sea Climate Atlas, Volume II, published by the U.S. Bureau of Land Management, estimates the maximum 100-year wind at 110 knots, and the extreme wave at 42.5 meters (136 feet). This wave-height estimate is thought to be excessive. The water depth, short fetch, and changeable winds will probably limit wave heights to less than half of this figure. The wind in this part of the world does not blow steadily in one direction at high velocity long enough to build waves this big.

Access

Getting to the Navarin basin is difficult and expensive. Reeve Aleutian Airways operates scheduled passenger and cargo service with Lockheed Electras and YS-11's among Anchorage, Dutch Harbor, St. Paul, and Adak. These places are still a long way from the Navarin Basin. Wien Air Alaska operates Boeing 727's among Seattle, Anchorage, Kodiak, Nome and other western Alaskan towns.

Sea access from the U.S. to the Navarin basin is via Unimak Pass, around the western end of Unimak Island. Unimak Pass is 3040 kilometers (1890 miles) from Seattle and about 1130 kilometers (700 miles) from Navarin basin.

REFERENCES

Agapitov, D. I., Burlin, Yu. K., Drabkin, N. Ye, and others, 1970, Results of the geological exploration for oil and gas in the Anadyr basin and goals in connection with future investigations: Geologiya Nefti i Gaza, no. 8, p. 22-25 (in Russian).

Agapitov, D. I., Vakhrushkin, P. A., and Ivanov, V. V., 1971, Neogene sediment of the southern part of the Anadyr basin: Geology and Geophysics, v. 8, p. 110-113.

Aleksandrov, A. A., 1973, Serpentinite melange in the upper course of the Chirynay River, Koryak Highlands: Geotectonika, v. 4, p. 84-93 (in Russian).

Aleksandrov, A. A., Bogdanov, N. S., Byalobzheskiy, S. G., Markov, M. S., Tilman, S. M., Khain, V. Ye., and Chekhov, A. D., 1976, New data on the tectonics of the Koryak highlands: Geotectonics, v. 9, p. 292-299. Geotectonics, no. 3, p. 148-154.

Askren, D. R., 1972, Holocene stratigraphic framework southern Bering Sea continental shelf: Univ. of Washington, MS Thesis, 104 p.

Bailey, E. H., and Blake, M. C., Jr., 1969, Tectonic development of western California during the late Mesozoic: Geotectonics, no. 3, p. 148-154; no. 4, p. 225-230.

Bailey, E. H., Irwin, W. P., and Jones, D. L., 1964, Franciscan and related rocks, and their significance in the geology of western California: California Division of Mines and Geology Bull. 183, 177 p.

Beikman, H. M., compiler, 1974, Preliminary geologic map of the southwest quadrant of Alaska: U.S. Geol. Survey Misc. Field Studies Map MF-611, 2 sheets.

Brockway, R., Alexander, B., Day, P., Lyle, W., Hiles, R., Decker, W., Polski, W., and Reed, B., 1975, Bristol Bay region, "Stratigraphic correlation section", southwest Alaska: The Alaska Geological Society, P. O. Box 1288, Anchorage, AK 99510.

Brower, W. A., Jr., Searby, H. W., Wise, J. L., Diaz, H. F., and Prechtel, A. S., 1977, Climatic atlas of the Outer Continental Shelf waters and coastal regions of Alaska, vol. II, Bering Sea: U.S. National Oceanic and Atmospheric Administration OCSEAP Final Report-RU 347, 443 pp.

Burk, C. A., 1965, Geology of the Alaska Peninsula Island arc and continental margin: Geol. Soc. America Mem. 99, 250 p.

Burlin, Yu. K., and others, 1975, Sedimentary basins of the far east and the northeast of the U.S.S.R. and their possible oil and gas content: 9th World Petroleum Cong., Tokyo, Proc., v. 3, p. 39-50.

Churkin, M., 1970, Fold belts of Alaska and Siberia and drift between North America and Asia: Proc. Geol. Seminar on the North Slope of Alaska, Pacific Sec., Am. Assoc. Petroleum Geologists, G1-G17.

Clark, S. H. B., 1973, The McHugh Complex of south-central Alaska: U.S. Geol. Survey Bull. 1372-D, p. D1-D11.

Coats, R. R., 1950, Volcanic activity in the Aleutian arc: U.S. Geol. Survey Bull. 974-B, p. 35-47.

Connelly, W., 1978, The Uyak Complex Kodiak Islands, Alaska; a Cretaceous subduction complex: Geol. Soc. America Bull., v. 89, p. 755-769.

Cooper, A. K., Scholl, D. W., Marlow, M. S., and others, 1979; Hydrocarbon potential of Aleutian Basin, Bering Sea: Am. Assoc. Pet. Geol. Bull., v. 63, p. 2070-2087.

Cooper, A. K., Bailey, K. A., Howell, J. I., Marlow, M. S., and Scholl, D. W., 1976a, Preliminary residual magnetic map of the Bering Sea basin and the Kamchatka Peninsula: U.S. Geol. Survey Misc. Field Studies Map MF-715, scale 1:2,500,000.

Cooper, A. K., Scholl, D. W., and Marlow, M. S., 1976b, Mesozoic magnetic lineations in the Bering Sea marginal basin: Jour. Geophys. Research, v. 81, p. 1916-1935.

Cooper, A. K., Scholl, D. W., and Marlow, M. S., 1976c, Plate tectonic model for the evolution of the Bering Sea basin: Geol. Soc. Amer. Bull., v. 87, p. 1119-1126.

Ernst, W. G., 1970, Tectonic contact between the Franciscan melange and the Great Valley sequence -- crustal expression of a Late Mesozoic Benioff zone: Jour. Geophys. Research, v. 75: p. 886-902.

Ewing, M., Ludwig, W. J., and Ewing, J., 1965, Oceanic structural history of the Bering Sea: Jour. Geophys. Research, v. 70, p. 4593-4600.

Gates, G. O., and Gryc, George, 1963, Structure and tectonic history of Alaska, in Backbone of the Americas: AAPG Mem. 2, p. 264-277.

Hamilton, W., 1969, Mesozoic California and the underflow of Pacific mantle. Geol. Soc. America Bull., v. 80, p. 2409-2430.

Hein, J. R., and others, 1978, Diagenesis of late Cenozoic diatomaceous deposits and formation of the bottom simulating reflector in the southern Bering Sea: Sedimentology, v. 25, p. 155-181.

Hoare, J. M., 1961, Geology and tectonic setting of lower Kuskokwim-Bristol Bay region, Alaska: Am. Assoc. Petroleum Geologists Bull., v. 45, no. 5, p. 594-611.

Hopkins, D. M., Scholl, D. W. Addicott, W., Pierce, R. L., Smith, P. B., Wolfe, J. A., Gershanovich, D., Kotenev, B., Lohman, K. E., Lipps, J. H., and Obradovich, J., 1969, Cretaceous Tertiary and early Pleistocene rocks from the continental margin in the Bering Sea: Geol. Soc. America Bull., v. 80, p. 1471-1480.

Jones, D. L., Silberling, N. J., and Hillhouse, J. W., 1978, Microplate tectonics of Alaska-significance for the Mesozoic history of the Pacific coast of North America, in Howell, D. G., and McDougall, K. A., eds., Mesozoic paleogeography of the Western United States: United States Pacific Coast

Paleogeography Symposium, 2d, Sacramento, April 29, 1978, Proc., p. 71-74.

Komar, P. D., Neudeck, R. H., and Kulm, L. D., 1972, Observations and significance of deep-water oscillatory ripple marks on the Oregon continental shelf, in Swift, D. J. P., Duane, D. B., and H. Pilkey, O. H., eds., Shelf sediment transport; Process and pattern: Stroudsbourg, Pa., Dowden, Hutchinson and Ross, Inc., p. 601-619.

Kvenvolden, K. A., and Redden, G. D., 1980, Hydrocarbon gas in sediment from the shelf, slope, and basin of the Bering Sea: Geochimica et Cosmochimica Acta, v. 44, p. 1145-1150.

Lisitsyn, A. P., 1966, Recent sedimentation in the Bering Sea (in Russian): Inst. Okeanol. Ahoc. Nauk USSR, (translated by Israel Program for Scientific Translation, available from U.S. Dept. Commerce, Clearinghouse for Fed. Sci. and Tech. Info., 1969, 614 pp.)

Lyle, W. M., Morehouse, J. A., Palmer, I. F., Jr., and Bolm, J. G., 1979, Tertiary formations and associated Mesozoic rocks in the Alaska Peninsula area, Alaska, and their petroleum-rservoir and source-rock potential: State of Alaska, Division of Geological and Geophysical Surveys, Geologic Report 62, 65 p.

Marlow, M. S., 1979, Hydrocarbon prospects in Navarin basin province, northwest Bering Sea shelf: Oil and Gas Journal, Oct. 29, p. 190-196.

Marlow, M. S., and Cooper, A. K., 1980, Mesozoic and Cenozoic structural trends beneath the southern Bering Sea shelf: AAPG Bull., v. 64, p. 2139-2155.

Marlow, M. S., Scholl, D. W., Cooper, A. K., and Buffington, E. C., 1976, Structure and evolution of Bering Sea shelf south of St. Lawrence Island: AAPG Bull., v. 60, no. 2, p. 161-183.

Marlow, M. S., Cooper, A. K., Scholl, D. W., Vallier, T. L., and McLean, Hugh, 1979a, Description of dredge samples from the Bering Sea continental margin: U.S. Gelogical Survey Open-File Report 79-1139, 5 p.

Marlow, M. S., Gardner, J. V., Vallier, T. L., McLean, H., Scott, E. W., and Lynch, M. B., 1979b, Resource report for proposed OCS sale No. 70, St. George basin, Alaska: U.S. Geological Survey Open-File Report 79-1650, 79 p.

Marlow, M. S., Scholl, D. W., Cooper, A. K., and Jones, D. L., 1979c, Shallow-water Upper Jurassic rocks dredged from Bering

Sea continental margin: American Association of Petroleum Geologists Bull., v. 63, no. 3, p. 490-491.

McLean, H., 1979a, Review of petroleum geology of Anadyr and Khgatyrka basins, USSR: AAPG Bull., v. 63, p. 1467-1477.

McLean, H., 1979b, Pribilof segment of the Bering Sea continental margin: a reinterpretation of Upper Cretaceous dredge samples: Geology, v. 7, p. 307-310.

McRoy, C. P., and Goering J. J., 1974, The influence of ice on the primary productivity of the Bering Sea, in Hood, D. W., and Kelley, E. J., eds., Oceanography of the Bering Sea with emphasis on renewable resources: Institute of Marine Science, University of Alaska, Fairbanks, Alaska, p. 403-419.

Meyerhoff, A. A., 1972, Russians look hard at the Anadyr basin: Oil and Gas Journal, v. 70, no. 43, pt. I, p. 124-129; no. 44, pt. II, p. 84-89.

Meyers, H., 1976, A historical summary of earthquake epicenters in and near Alaska: U.S. National Oceanic and Atmospheric Administration Tech. Memorandum EDS NGSDC-1, 80 p.

Page, B. M., 1970, Sur-Nacimiento fault zone of California: Geol. Soc. America Bull., v. 81, p. 667-690.

Page, B. M., 1978, Franciscan melanges compared with olistostromes of Taiwan and Italy: Tectonophysics, v. 47, p. 223-246.

Patton, W. W., Jr., 1973, Reconnaissance geology of the northern Yukon-Koyukuku Province, Alaska: U.S. Geol. Survey Prof. Paper 774-A, 17 p.

Patton, W. W., Jr., Lanphere, M. A., Miller, T. P., and Scott, R. A., 1976, Age and tectonic significance of volcanic rocks on St. Matthew Island, Bering Sea, Alaska: U.S. Geological Survey Jour. of Research, v. 4, p. 67-74.

Patton, W. W., Jr., and Csejtey, Bela, Jr., 1971, Preliminary geologic investigations of western St. Lawrence Island, Alaska: U.S. Geological Survey Professional Paper 684-C, p. C1-C15.

Payne, T. G., compiler, 1955, Mesozoic and Cenozoic tectonic elements of Alaska: U.S. Geol. Survey Misc. Geol. Inv. Map I-84, scale 1:5,000,000.

Pratt, R., Rutstein, M. S., Walton, F. W., and Buschur, J. A., 1972, Extension of Alaskan structural trends beneath Bristol Bay, Bering shelf, Alaska: Jour. Geophys. Res., v. 77, p. 4994-4999.

Review of Sino-Soviet Oil, 1974, The prospects of the Anadyr and Khatyrka basins: v. 9, no. 11, p. 6-16.

Rovnin, L. I., Dvurechensikiy, V. A., and Ovcharenko, A. V., 1976, Results of geological exploration work on oil and gas by the Ministry of Geology-USSR, from 1971-1975 and the main trend in the tenth five year plan: Geologiya Nefti i Gaza, no. 7, p. 1-7 (in Russian).

Scholl, D. W., Buffington, E. C., and Marlow, M. S., 1975, Plate tectonics and the structural evolution of the Aleutian-Bering Sea region, in Forbes, R. B., ed., Contributions to the geology of the Bering Sea basin and adjacent regions: Geol. Soc. America Spec. Paper 151, p. 1-32.

Scholl, D. W., and Cooper, A. K., 1978, VAMPs: Possible hydrocarbon-bearing structures in Bering Sea basin: AAPG Bull., v. 62, p. 2481-2488.

Scholl, D. W., Cooper, A. K., Marlow, M. S., and others, 1979, Hydrocarbon potential of Aleutian Basin, Bering Sea: Am. Assoc. of Pet. Geol. Bull., v. 63, no. 11 (Part I of II).

Scholl, D. W., and Creager, J. S., 1973, Geologic synthesis of Leg 19 (DSDP) results: far North Pacific, Aleutian Ridge and

Bering Sea, in Initial reports of the Deep Sea Drilling Project, v. 19: Washington, D.C., U.S. Govt. Printing Office, p. 897-913.

Scholl, D. W., Marlow, M. S., Creager, J. S., Holmes, M. L., Wolf, S. C., and Cooper, A. K., 1970, A search for the seaward extension of the Kaltag fault beneath the Bering Sea: Geological Society of America Abstracts with Programs, v. 2, p. 141-142.

Shipley, Thomas H., Houston, Mark H., Buffler, Richard T., Shaub, F. Jeanne, McMillen, Kenneth J., Ladd, John W., and Worzel, J. Lamar, 1979, Seismic evidence for widespread possible gas hydrate horizons on continental slopes and rises: American Assoc. of Petroleum Geol. Bull., v. 63, no. 12, Dec. 1979.

Silver, E. A., and Beutner, E. C., 1980, Melanges: Geology, v. 8, p. 32-34.

Trofimuk, A. A., 1971, Oil and gas prospective basins of the Far East, USSR: Moscow, Nedra, 183 p. (in Russian).

Tysdal, R. G., and Case, J. E., 1976, The McHugh Complex in the Seward quadrangle, south-central Alaska, in Blean, K. M., The United States Geological Survey in Alaska; Accomplishments during 1976: U.S. Geological Survey Circular 751-B, p. B48-B49.

Tysdal, R. G., Case, J. E., Winkle, G. R., and Clark, S. H. B., 1977, Sheeted dikes, gabbro, and pillow basalt in flysch of coastal southern Alaska: Geology, v. 5, p. 377-383.

Vallier, T. L., Underwood, M. B., Jones, D. L., and Gardner, J. V., 1979, Petrography and geological significance of upper Jurassic rocks dredged near Pribilof Islands, southern Bering Sea continental shelf: AAPG Bull., v. 64, p. 945-950.

Varnes, D. J., 1978, Slope movement types and process, in Schuster, R. L., and Krizek, R. J., eds., Landslides, analysis and control: Washington, D. C., Natl. Acad. of Sciences, p. 11-33.

Verba, M. L., Gaponenko, G. I., Ivanov, S. S., Orlov, A. N., Timofeev, V. I., and Cherenkov, Iu. F., 1971, Glubinnoe stroesue i perspektivy neftigazonosnosti severo-zapadnoi chasti beringova moria-V sb (Deep structure of northwestern part of the Bering Sea and the prospects of finding oil and gas): Geofizicheskie metody razvedki v Arktike L, Niiga, vyp 6, p. 70-74.

Vogel, T. M., Kvenvolden, K. A., Carlson, P. R., and Karl, H. A., 1981, Geochemical prospecting for hydrocarbons in the Navarin basin province: American Association of Petroleum Geologists Bulletin, v. 65, no. 4 (in press).

Yanshin, A. L., ed., 1966, Tectonic map of Eurasia: Geol. Inst. Acad. Sci. USSR., Moscow (in Russian), scale 1:5,000,000.

Figure Captions

Figure 1. Location of proposed OCS (Outer Continental Shelf) Lease Sale #83 in the northern Bering Sea. Albers equal area projection.

Figure 2. Trackline chart of 24-channel seismic-reflection profiles across the Navarin basin province. High-resolution seismic-reflection, refraction, bathymetry, gravity, and limited magnetic data were also collected along the tracklines. Navarin basin province shown by stipple pattern. Albers equal area projection.

Figure 3. Generalized geologic map of western Alaska, the Alaska Peninsula, and eastern Siberia. Onshore geology is modified from Burk (1965), Beikman (1974), and Yanshin (1966).

Figure 4. Location map of selected cross sections across the Navarin basin province and easter Siberia shown in Figures 5, 6, and 7. Note also outline of proposed lease area. Albers equal area projection.

Figure 5. Generalized cross section across the Koryak Range in eastern Siberia. Adapted from Aleksandrov and others (1976) and McLean (1979a).

Figure 6. Interpretive drawing of seismic-reflection profile A-B across the Navarin basin province. Free-air gravity profile shown at top. Vertical kilometer scale shown at right is applicable only to the shelf portion of the profile. Vertical time scale is two-way travel time. For location of profile see Figure 4.

Figure 7. Interpretive drawing of seismic-reflection profile C-D across the Navarin basin province. Free-air gravity profile shown at top. Vertical time scale is two-way travel time. For location of profile see Figure 4.

Figure 8. Structure contour map of acoustic basement in the Navarin basin province. See text for details of derivation. Albers equal area projection.

Figure 9. Location map of Anadyr and Khatyrka basins in eastern Siberia in relation to the Navarin basin. Albers equal area projection.

Figure 10. Location of dredge sites along the Bering Sea continental margin in relation to the Navarin basin province. Location of site #TT-1-021 is from Hopkins and others (1969) and locations of sites #DR-1-20, 26 are from Vallier and others (1979). Remaining sites are described in Marlow and others (1979a) and Marlow and Cooper (1980). Navarin basin province shown by stippled pattern. Albers equal area projection.

Figure 11. Location map for seismic profiles shown in figures 12 and 13.

Figure 12. Seismic profiles B99 and L4 collected along the slope areas of the Navarin basin province. The profiles show two BSRs, one at the base of a gas hydrate zone (BSR-GH) and one at a silica-diagenetic boundary (BSR-DB). See figure 11 for location.

Figure 13. Seismic profiles L13 and L46 collected along the slope areas in and around the Navarin basin province. The profiles show two BSRs, one at the base of a gas hydrate zone (BSR-GH) and one at a silica-diagenetic boundary (BSR-DB). See figure 11 for location.

Figure 14. Preliminary map of fault traces and areas of gas-charged sediment in Navarin basin province. Lines of fault trace are drawn at right angles to line of seismic profiles. Bathymetry in meters.

Figure 15. Preliminary map of identified areas of submarine landslides and sediment waves in Navarin basin province. Bathymetry in meters.

Figure 16. Preliminary map of sediment types in Navarin basin province derived from visual inspection of core samples onboard ship. Mean grain diameter (m) listed at those stations for which samples have been analyzed. Bathymetry in meters.

Figure 17. Outline of proposed OCS Lease Sale #83 (including Navarin basin province) and generalized isopach map of sediment thickness above "acoustic basement." Based in part on Figure 8. Areas with sediment thickness greater than 2 kilometers are considered most prospective for hydrocarbon accumulations. Albers equal area projection.